

## Accepted Manuscript

Dioxidomolybdenum(VI) complexes bearing sterically constrained aroylazine ligands: Synthesis, structural investigation and catalytic evaluation

Sudarshana Majumder, Sagarika Pasayat, Satabdi Roy, Subhashree P. Dash, Sarita Dhaka, Mannar R. Maurya, Martin Reichelt, Hans Reuter, Krzysztof Brzezinski, Rupam Dinda

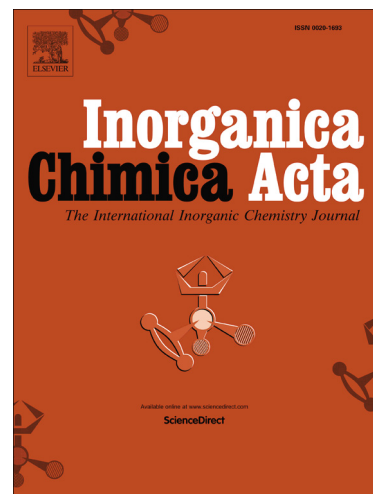
PII: S0020-1693(17)31047-2  
DOI: <http://dx.doi.org/10.1016/j.ica.2017.09.043>  
Reference: ICA 17902

To appear in: *Inorganica Chimica Acta*

Received Date: 5 July 2017  
Revised Date: 15 September 2017  
Accepted Date: 15 September 2017

Please cite this article as: S. Majumder, S. Pasayat, S. Roy, S.P. Dash, S. Dhaka, M.R. Maurya, M. Reichelt, H. Reuter, K. Brzezinski, R. Dinda, Dioxidomolybdenum(VI) complexes bearing sterically constrained aroylazine ligands: Synthesis, structural investigation and catalytic evaluation, *Inorganica Chimica Acta* (2017), doi: <http://dx.doi.org/10.1016/j.ica.2017.09.043>

This is a PDF file of an unedited manuscript that has been accepted for publication. As a service to our customers we are providing this early version of the manuscript. The manuscript will undergo copyediting, typesetting, and review of the resulting proof before it is published in its final form. Please note that during the production process errors may be discovered which could affect the content, and all legal disclaimers that apply to the journal pertain.



**Dioxidomolybdenum(VI) complexes bearing sterically constrained aroylazine ligands:  
Synthesis, structural investigation and catalytic evaluation**

Sudarshana Majumder<sup>a</sup>, Sagarika Pasayat<sup>a</sup>, Satabdi Roy<sup>a</sup>, Subhashree P. Dash<sup>a,b</sup>, Sarita Dhaka<sup>c,d</sup>, Mannar R. Maurya<sup>d</sup>, Martin Reichelt<sup>e</sup>, Hans Reuter<sup>e</sup>, Krzysztof Brzezinski<sup>f</sup>, Rupam Dinda\*<sup>a</sup>

<sup>a</sup>*Department of Chemistry, National Institute of Technology, Rourkela 769008, Odisha, India*

<sup>b</sup>*Department of Basic Sciences, Parala Maharaja Engineering College, Sitalapalli, Brahmapur, Odisha 761003, India*

<sup>c</sup>*Central Scientific Instruments Organisation (CSIR-CSIO), Sector 30 C, Chandigarh 160030, India*

<sup>d</sup>*Department of Chemistry, Indian Institute of Technology Roorkee, Roorkee 247667, India*

<sup>e</sup>*Institute of Chemistry of New Materials, University of Osnabrück, Barbarastrasse 7, 49067 Osnabrück, Germany*

<sup>f</sup>*Institute of Chemistry, University of Białystok, Ciołkowskiego 1K, 1 15-245 Białystok, Poland*

---

**Abstract**

Seven new dioxidomolybdenum(VI) complexes  $[\text{MoO}_2\text{L}^1(\text{X})]\cdot\text{X}$  (**1**) and  $[\text{MoO}_2\text{L}^{2-7}(\text{X})]$  (**2–7**) [Where X= EtOH in case of **1** and **5** and X=DMSO in case of **2–4** and **6, 7**] of aroylazines containing a bulky 3-hydroxy-2-naphthoic substituent, were isolated and structurally characterized. The aroylazine ligands  $\text{H}_2\text{L}^{1-7}$  were derived from the condensation of 3-hydroxy-2-naphthoic acid hydrazide with several substituted aromatic aldehydes/ketones. All the synthesized ligands and metal complexes were successfully characterized by elemental analysis, IR, UV–Vis and NMR spectroscopy. X-ray structures of **1–6** revealed that the ligands coordinate to the metal center as a dibasic tridentate ligand. Cyclic voltammetry of the complexes shows two irreversible reductive responses within the potential window  $-0.50$  to  $-1.36$  V, due to  $\text{Mo}^{\text{VI}}/\text{Mo}^{\text{V}}$  and  $\text{Mo}^{\text{V}}/\text{Mo}^{\text{IV}}$  processes. The synthesized complexes **1–7** were used as catalysts for the oxidation of benzoin, and for the oxidative bromination of salicylaldehyde, as a functional mimic of haloperoxidase. It was found that the percentage of conversion increased significantly in the presence of catalysts **1–7** which contained bulky substituents, and showed high percentage of conversion ( $>90\%$ ) with high turnover frequency ( $>1100$   $\text{h}^{-1}$ ) than previously reported catalysts. Benzil, benzoic acid and benzaldehyde-dimethylacetal were formed selectively for the oxidation of benzoin. Formation of 5-bromosalicylaldehyde and 3,5-dibromosalicylaldehyde took place during the oxidative bromination of salicylaldehyde in presence of  $\text{H}_2\text{O}_2$  as an oxidant and therefore **1–7** act as functional models of vanadium dependent haloperoxidases.

---

*Keywords:* Aroylazines / dioxidomolybdenum(VI) / X-ray crystallography / oxidation of benzoin / oxidative bromination of salicylaldehyde

## 1. Introduction

The chemistry of dioxidomolybdenum(VI) complexes has continued to attract the attention of researchers owing to its versatile reactivity [1,2] and biochemical [3–7] and catalytic [8–12] significance. The presence of molybdenum-oxido bonds in various molybdoenzymes [13–15, 16, 17] has stimulated research on molybdenum complexes with oxygen environments [2, 18–21], and in this aspect molybdenum Schiff-base complexes have gained substantial importance in recent times [18, 22–26]. In particular, aroylazines containing azomethine group ( $-\text{C}=\text{N}-\text{N}=\text{C}-$ ) [27–29], constitute an interesting category of such ligands as they have the potential to stabilize metal ions in different oxidation states [27–31] and can therefore tune the molecular architecture and geometry [32] of complexes. Further, the donor/acceptor abilities, electronic properties and steric strain factors of ligands influence the catalytic potential of the complexes [32–37] as evidenced in various reactions catalysed by molybdenum complexes [8, 36–41]. Such reactions catalysed by molybdenum complexes include the isomerization of allyl alcohols [42], olefin metathesis [43], oxo transfer reactions [44–46], ammoxidation of propylene [47] and epoxidation of alkenes [48].

On another hand, oxidation of  $\alpha$ -hydroxy ketones to  $\alpha$ -diketones belong to one of the most significant classes of organic transformations [49,50]. The dicarbonyl compounds like benzils, obtained from oxidation of benzoin, can further be employed in the synthesis of biologically active organic molecules [51–54] and as photosensitive agents. Although several oxidizing agents like chromium oxide [55,56], nitric acid [57], ammonium nitrate–copper acetate [58], thallium nitrate [59], triarylstibanes [60], etc. have been explored for catalysing these reactions, the search of versatile reagents is still prevalent for the development of convenient and selective procedures. However, very few reports of oxidomolybdenum complexes catalysed benzoin oxidation reactions are available in the literature [32, 60–63].

Additionally, haloperoxidase reactions are environmentally benign procedures for brominating organic compounds [64–67]. Haloperoxidase enzymes catalyse the oxidation of halide ions by hydrogen peroxide [66–68] and yield halogenated organic substrates which have pharmacological significance due to their antifungal, antibacterial, antineoplastic, antiviral and anti-inflammatory properties [67,69–71]. There has been extensive studies on oxidovanadium(V) complexes which can act as haloperoxidase mimics and several vanadium dependant bromoperoxidase models have been established [72–81]. However, reports of oxidomolybdenum(VI) haloperoxidase models are scanty [32,63,82,83] and seek further exploration.

As a part of our continuing interest in oxidometal complexes of aroylazines in relation to their biological [84–92] and catalytic [32,84,93] applications, herein we report seven dioxidomolybdenum(VI) complexes  $[\text{MoO}_2\text{L}^1(\text{X})]\cdot\text{X}$  (**1**) and  $[\text{MoO}_2\text{L}^{2-7}(\text{X})]$  (**2–7**) [Where X= EtOH in case of **1** and **5** and X=DMSO in case of **2–4** and **6, 7**] of aroylazine ligands  $\text{H}_2\text{L}^{1-7}$  (**Scheme 1**). Earlier we had explored the catalytic potential of dioxidomolybdenum(VI) complexes of similar aroylazines where fair catalytic results were obtained [32]. To improve the catalytic efficiency, a bulky 3-hydroxy-2-naphthoic substituent has now been introduced in aroylazine ligands to observe its influence, if any, on the catalytic potential of the reported complexes. All the complexes have been characterized by several physicochemical techniques (IR, UV–Vis, NMR and ESI-MS) and the crystal structures of  $[\text{MoO}_2\text{L}^1(\text{EtOH})]\cdot\text{EtOH}$  (**1**),  $[\text{MoO}_2\text{L}^2(\text{DMSO})]$  (**2**),  $[\text{MoO}_2\text{L}^3(\text{DMSO})]$  (**3**),  $[\text{MoO}_2\text{L}^4(\text{DMSO})]$  (**4**),  $[\text{MoO}_2\text{L}^5(\text{EtOH})]$  (**5**) and  $[\text{MoO}_2\text{L}^6(\text{DMSO})]$  (**6**) have been determined by X-ray crystallography. The catalytic activity of **1–7** for the oxidation of benzoin, and for the oxidative bromination of salicylaldehyde, as a functional mimic of haloperoxidase has been explored. Significant percentage of conversion (>90%) was obtained

in the presence of catalysts **1–7**, and better selectivity of products and high turnover frequency ( $>1100 \text{ h}^{-1}$ ) was achieved in comparison to previously reported catalysts [32,60,63,82,83]. During the oxidation of benzoin, benzil, benzoic acid and benzaldehyde-dimethylacetal were formed selectively. Also, selective formation of 5-bromosalicylaldehyde and 3,5-dibromosalicylaldehyde took place during the oxidative bromination of salicylaldehyde in presence of  $\text{H}_2\text{O}_2$  as an oxidant and therefore **1–7** acted as functional models of vanadium dependent haloperoxidases.

## 2. Experimental Section

### 2.1. Materials and methods

[MoO<sub>2</sub>(acac)<sub>2</sub>] was prepared as described in the literature [94]. Reagent grade solvents were dried and distilled prior to use. All other chemicals were reagent grade, available commercially and used as received. Elemental analyses were performed on a VarioELcube CHNS Elemental analyzer. IR spectra were recorded on a Perkin-Elmer Spectrum RXI spectrometer. NMR spectra were recorded with a Bruker Ultrashield 400 MHz spectrometer at 298 K room temperature using SiMe<sub>4</sub> (<sup>1</sup>H and <sup>13</sup>C) as an internal. Electronic spectra were recorded on a Lamda25, PerkinElmer spectrophotometer. Mass spectra were recorded on an SQ-300 MS instrument operating in ESI mode. Magnetic susceptibility was measured with a Sherwood Scientific AUTOMSB sample magnetometer. Conductivity was measured using Eutech CON 700 conductivity meter. A CH-Instruments (Model No. CHI6003E) electrochemical analyzer was used for cyclic voltammetric experiments with CH<sub>3</sub>CN solutions of the complexes containing TBAP (tetra butyl ammonium perchlorate) as the supporting electrolyte. The three electrode measurements were carried out at 298 K with a glassy carbon working electrode, platinum auxiliary electrode, and Ag/AgCl as a reference electrode. CAUTION: Although no problems were encountered during the course of this work, attention is drawn to the potentially explosive nature of perchlorates.

A Shimadzu 2010 plus gas-chromatograph fitted with a Rtx-1 capillary column (30 m × 0.25 mm × 0.25 μm) and a FID detector was used to analyse the reaction products and their quantifications were made on the basis of the relative peak area of the respective product. The identity of the products was confirmed using a GC-MS model Perkin-Elmer, Clarus 500 and comparing the fragments of each product with the library available. The percent conversion of substrate and selectivity of products was calculated from GC data using the formulae:

$$\% \text{ Conversion of substrate} = 100 - \frac{\text{Peak area of a substrate}}{\text{Total area of substrate} + \text{products}} \times 100$$

$$\% \text{ Selectivity of a product} = \frac{\text{Peak area of a product}}{\text{Total area of products}} \times 100$$

## 2.2. Synthesis of Ligands ( $H_2L^{1-7}$ )

The aroylazine ligands,  $H_2L^{1-7}$ , were prepared by the condensation of 3-hydroxy-2-naphthoic hydrazide with the corresponding aldehydes and ketones (salicylaldehyde, *o*-vanillin, 5-bromosalicylaldehyde, 2-hydroxy-1-naphthaldehyde, 2'-hydroxyacetophenone, 2'-hydroxy-4'-methoxyacetophenone and 2-hydroxy-5-methoxybenzaldehyde, respectively) following a standard procedure [32]. The resulting light brown compounds were filtered, washed with ethanol and dried over fused  $CaCl_2$ .

$H_2L^1$ : Yield: 0.21 g (68%). Anal. Calcd for  $C_{18}H_{14}N_2O_3$ : C, 70.58; H, 4.61; N, 9.15. Found: C, 70.54; H, 4.59; N, 9.10 %. FTIR (KBr,  $\nu_{max}/cm^{-1}$ ):  $\nu(O-H)$  3540, 3488,  $\nu(N-H)$  3003,  $\nu(C=O)$  1645,  $\nu(C=N)$  1614.  $^1H$  NMR (400 MHz, DMSO- $d_6$ ):  $\delta$  (ppm) = 12.15 (s, 1H, -NH), 11.22 (s, 2H, -OH), 8.69 (s, 1H, -CH), 8.47–6.92 (m, 10H, aromatic).  $^{13}C$  NMR (100 MHz, DMSO- $d_6$ ):  $\delta$  (ppm) = 164.09, 157.99, 154.53, 149.36, 136.39, 132.09, 130.79, 129.95, 129.14, 128.78, 127.24, 126.33, 124.31, 120.39, 119.88, 119.12, 116.93, 111.08.

$H_2L^2$ : Yield: 0.22 g (64%). Anal. Calcd for  $C_{19}H_{16}N_2O_4$ : C, 67.85; H, 4.79; N, 8.33. Found: C, 67.81; H, 4.72; N, 8.30 %. FTIR (KBr,  $\nu_{max}/cm^{-1}$ ):  $\nu(O-H)$  3554, 3465,  $\nu(N-H)$ , 3005,  $\nu(C=O)$  1648,  $\nu(C=N)$  1610.  $^1H$  NMR (400 MHz, DMSO- $d_6$ ):  $\delta$  (ppm) = 11.94 (s, 1H, -NH), 10.92 (s, 2H, -OH), 8.69 (s, 1H, -CH), 8.45–6.86 (m, 9H, aromatic), 3.82 (s, 3H, -OCH<sub>3</sub>).  $^{13}C$  NMR (100 MHz, DMSO- $d_6$ ):  $\delta$  (ppm) = 164.05, 154.45, 149.12, 148.41, 147.64, 136.34,

130.79, 129.14, 128.79, 126.31, 124.32, 121.16, 120.53, 119.61, 119.34, 114.39, 114.02, 56.28.

H<sub>2</sub>L<sup>3</sup>: Yield: 0.27 g (70%). Anal. Calcd for C<sub>18</sub>H<sub>13</sub>BrN<sub>2</sub>O<sub>3</sub>: C, 56.12; H, 3.40; N, 7.27. Found: C, 56.15; H, 3.42; N, 7.23 %. FTIR (KBr,  $\nu_{\max}/\text{cm}^{-1}$ ):  $\nu(\text{O-H})$  3543, 3398,  $\nu(\text{N-H})$  3008,  $\nu(\text{C=O})$  1649,  $\nu(\text{C=N})$  1612. <sup>1</sup>H NMR (400 MHz, DMSO-d<sub>6</sub>):  $\delta$  (ppm) = 11.99 (s, 1H, -NH), 11.28 (s, 2H, -OH), 8.21 (s, 1H, -CH), 7.92–6.92 (m, 9H, aromatic). <sup>13</sup>C NMR (100 MHz, DMSO-d<sub>6</sub>):  $\delta$  (ppm) = 164.22, 156.92, 154.39, 146.62, 136.34, 134.27, 130.84, 129.14, 128.81, 127.21, 126.31, 124.32, 121.71, 120.61, 119.18, 111.00, 110.97.

H<sub>2</sub>L<sup>4</sup>: Yield: 0.22 g (62%). Anal. Calcd for C<sub>22</sub>H<sub>16</sub>N<sub>2</sub>O<sub>3</sub>: C, 74.15; H, 4.53; N, 7.86. Found: C, 74.16; H, 4.51; N, 7.82 %. FTIR (KBr,  $\nu_{\max}/\text{cm}^{-1}$ ):  $\nu(\text{O-H})$  3548, 3421,  $\nu(\text{N-H})$  3007,  $\nu(\text{C=O})$  1645,  $\nu(\text{C=N})$  1614. <sup>1</sup>H NMR (400 MHz, DMSO-d<sub>6</sub>):  $\delta$  (ppm) = 12.80 (s, 1H, -NH), 12.25 (s, 1H, -OH), 11.36 (s, 1H, -OH), 9.57 (s, 1H, -CH), 8.53–7.28 (m, 12H, aromatic). <sup>13</sup>C NMR (100 MHz, DMSO-d<sub>6</sub>):  $\delta$  (ppm) = 163.49, 158.62, 154.32, 148.03, 136.41, 133.41, 132.16, 131.18, 129.42, 129.20, 128.84, 128.29, 128.24, 127.30, 126.35, 124.37, 124.06, 121.50, 120.44, 119.38, 111.07, 109.10.

H<sub>2</sub>L<sup>5</sup>: Yield: 0.19 g (61%). Anal. Calcd for C<sub>19</sub>H<sub>16</sub>N<sub>2</sub>O<sub>3</sub>: C, 71.24; H, 5.03; N, 8.74. Found: C, 71.21; H, 5.05; N, 8.71 %. FTIR (KBr,  $\nu_{\max}/\text{cm}^{-1}$ ):  $\nu(\text{O-H})$  3533, 3478,  $\nu(\text{N-H})$  3005,  $\nu(\text{C=O})$  1642,  $\nu(\text{C=N})$  1614. <sup>1</sup>H NMR (400 MHz, DMSO-d<sub>6</sub>): 13.24 (s, 1H, -NH), 11.75 (s, 2H, -OH), 8.62 – 6.91 (m, 10H, aromatic), 3.36 (s, 3H, -CH<sub>3</sub>). <sup>13</sup>C NMR (100 MHz, DMSO-d<sub>6</sub>):  $\delta$  (ppm) = 162.16, 159.00, 156.37, 153.10, 136.24, 132.58, 131.64, 129.29, 128.86, 128.76, 127.49, 126.13, 124.30, 120.58, 119.60, 118.99, 117.68, 111.01, 13.60.

H<sub>2</sub>L<sup>6</sup>: Yield: 0.23 g (65%). Anal. Calcd for C<sub>20</sub>H<sub>18</sub>N<sub>2</sub>O<sub>4</sub>: C, 68.56; H, 5.18; N, 8.00. Found: C, 68.54; H, 5.17; N, 8.05 %. FTIR (KBr,  $\nu_{\max}/\text{cm}^{-1}$ ):  $\nu(\text{O-H})$  3493, 3387,  $\nu(\text{N-H})$  3003,  $\nu(\text{C=O})$  1644,  $\nu(\text{C=N})$  1615. <sup>1</sup>H NMR (400 MHz, DMSO-d<sub>6</sub>):  $\delta$  (ppm) = 13.55 (s, 1H, -NH), 11.69 (s, 2H, -OH), 8.61– 6.49 (m, 9H, aromatic), 3.79 (s, 3H, -OCH<sub>3</sub>), 2.43 (s, 3H, -CH<sub>3</sub>).

$^{13}\text{C}$  NMR (100 MHz, DMSO- $d_6$ ):  $\delta$  (ppm) = 162.27, 162.04, 161.14, 156.78, 153.22, 136.28, 132.54, 130.25, 129.38, 128.83, 127.58, 126.24, 124.40, 120.74, 112.96, 111.06, 106.27, 102.06, 55.71, 13.74.

$\text{H}_2\text{L}^7$ : Yield: 0.24 g (72%). Anal. Calcd for  $\text{C}_{19}\text{H}_{16}\text{N}_2\text{O}_4$ : C, 67.85; H, 4.79; N, 8.33. Found: C, 67.83; H, 4.75; N, 8.32 %. FTIR (KBr,  $\nu_{\text{max}}/\text{cm}^{-1}$ ):  $\nu(\text{O-H})$  3556, 3433,  $\nu(\text{N-H})$ , 3004,  $\nu(\text{C=O})$  1646,  $\nu(\text{C=N})$  1614.  $^1\text{H}$  NMR (400 MHz, DMSO- $d_6$ ):  $\delta$  (ppm) = 12.16 (s, 1H, -NH), 11.34 (s, 1H, -OH), 10.65 (s, 1H, -OH), 8.66 (s, 1H, -CH), 8.46–6.88 (m, 9H, aromatic), 3.74 (s, 3H, -OCH<sub>3</sub>).  $^{13}\text{C}$  NMR (100 MHz, DMSO- $d_6$ ):  $\delta$  (ppm) = 164.07, 154.52, 152.58, 151.99, 148.36, 136.32, 130.73, 129.12, 128.73, 127.20, 126.33, 124.28, 120.64, 119.39, 118.99, 117.79, 112.33, 110.99, 55.93.

### 2.3. Synthesis of Complexes 1–7

$[\text{MoO}_2\text{L}^1(\text{EtOH})]\cdot\text{EtOH}$  (**1**): To the refluxing solution of ligand  $\text{H}_2\text{L}^1$  (1 mmol) in 30 mL ethanol,  $\text{MoO}_2(\text{acac})_2$  (1 mmol) was added. The color of the solution immediately turned red. After 3 h reflux, the solution was cooled, filtered and kept for crystallization. Slow evaporation of the filtrate for 2 days produced dark yellow crystals suitable for X-Ray analysis. Yield: 0.27 g (57 %). Anal. Calcd for  $\text{C}_{22}\text{H}_{24}\text{MoN}_2\text{O}_7$ : C, 50.39; H, 4.61; N, 5.34. Found: C, 50.37; H, 4.60; N, 5.32 %. FTIR (KBr,  $\nu_{\text{max}}/\text{cm}^{-1}$ ):  $\nu(\text{O-H})$  3361,  $\nu(\text{C=N})$  1601,  $\nu(\text{M=O})$  918, 910. UV-Vis (DMSO):  $\lambda_{\text{max}}$ , nm ( $\epsilon$ ,  $\text{dm}^3 \text{mol}^{-1} \text{cm}^{-1}$ ): 417 (1447), 331 (5540), 259 (6113).  $^1\text{H}$  NMR (400 MHz, DMSO- $d_6$ ):  $\delta$  (ppm) = 11.24 (s, 1H, -OH), 9.18 (s, 1H, -CH), 8.54–7.00 (m, 10H, aromatic), 4.43 (1H, OH, ethanol), 2.50 (q, 2H, -CH<sub>2</sub> ethanolic), 1.05 (t, 3H, -CH<sub>3</sub> ethanolic).  $^{13}\text{C}$  NMR (100 MHz, DMSO- $d_6$ ):  $\delta$  (ppm) = 208.57, 169.16, 159.74, 157.37, 154.58, 136.92, 136.00, 134.99, 131.52, 129.49, 129.23, 127.43, 126.39, 124.32, 122.54, 120.45, 119.14, 116.13, 111.36, 89.09. ESI-MS:  $m/z$  524.20  $[\text{M}]^+$ .

[MoO<sub>2</sub>L<sup>2</sup>(DMSO)] (**2**): To the refluxing solution of ligand H<sub>2</sub>L<sup>2</sup> (1 mmol) in 30 mL ethanol, MoO<sub>2</sub>(acac)<sub>2</sub> (1 mmol) was added. The color of the solution immediately turned red. After 3 h of reflux, the solution was cooled, filtered. The dark brown residue obtained was crystallized in DMSO. Slow evaporation of the solution for 2 days produced orange crystals suitable for X-Ray analysis. Yield: 0.31 g (58 %). Anal. Calcd for C<sub>21</sub>H<sub>20</sub>MoN<sub>2</sub>O<sub>7</sub>S: C, 46.67; H, 3.73; N, 5.18; S, 5.93. Found: C, 46.65; H, 3.77; N, 5.16; S, 5.90 %. FTIR (KBr,  $\nu_{\max}/\text{cm}^{-1}$ ):  $\nu(\text{O-H})$  3440,  $\nu(\text{C=N})$  1615,  $\nu(\text{M=O})$  940, 914. UV-Vis (DMSO):  $\lambda_{\max}$ , nm ( $\epsilon$ ,  $\text{dm}^3 \text{mol}^{-1} \text{cm}^{-1}$ ): 382 (1760), 333 (2853), 260 (3340). <sup>1</sup>H NMR (400 MHz, DMSO-d<sub>6</sub>):  $\delta$  (ppm) = 11.24 (s, 1H, -OH), 9.18 (s, 1H, -CH), 8.55–7.07 (m, 9H, aromatic), 3.83 (s, 3H, -OCH<sub>3</sub>), 2.50 (s, 6H, DMSO). <sup>13</sup>C NMR (100 MHz, DMSO-d<sub>6</sub>):  $\delta$  (ppm) = 169.18, 157.38, 154.60, 149.52, 148.90, 136.92, 131.52, 129.49, 129.23, 127.42, 126.40, 125.88, 124.31, 122.45, 120.71, 117.98, 116.14, 111.36, 56.36, 40.74. ESI-MS:  $m/z$  540.21 [M]<sup>+</sup>.

[MoO<sub>2</sub>L<sup>3</sup>(DMSO)] (**3**): To the refluxing solution of ligand H<sub>2</sub>L<sup>3</sup> (1 mmol) in 30 mL ethanol, MoO<sub>2</sub>(acac)<sub>2</sub> (1 mmol) was added. The color of the solution immediately turned red. After 3 h of reflux, the solution was cooled, filtered. The dark brown residue obtained was crystallized in DMSO. Slow evaporation of the solution for 2 days produced orange crystals suitable for X-Ray analysis. Yield: 0.32 g (55 %). Anal. Calcd for C<sub>20</sub>H<sub>17</sub>BrMoN<sub>2</sub>O<sub>6</sub>S: C, 40.76; H, 2.91; N, 4.75; S, 5.44. Found: C, 40.72; H, 2.89; N, 4.70; S, 5.41. %. FTIR (KBr,  $\nu_{\max}/\text{cm}^{-1}$ ):  $\nu(\text{O-H})$  3491,  $\nu(\text{C=N})$  1608,  $\nu(\text{M=O})$  933, 914. UV-Vis (DMSO):  $\lambda_{\max}$ , nm ( $\epsilon$ ,  $\text{dm}^3 \text{mol}^{-1} \text{cm}^{-1}$ ): 401 (3053), 336 (9933), 261 (11760). <sup>1</sup>H NMR (400 MHz, DMSO-d<sub>6</sub>):  $\delta$  (ppm) = 11.16 (s, 1H, -OH), 9.12 (s, 1H, -CH), 8.54–6.98 (m, 9H, aromatic), 2.50 (s, 6H, DMSO). <sup>13</sup>C NMR (100 MHz, DMSO-d<sub>6</sub>):  $\delta$  (ppm) = 169.65, 158.93, 156.19, 154.54, 137.99, 137.01, 136.45, 131.72, 129.53, 129.34, 127.44, 126.41, 124.37, 122.40, 121.51, 115.98, 113.16, 111.42, 40.76. ESI-MS:  $m/z$  589.50 [M]<sup>+</sup>.

[MoO<sub>2</sub>L<sup>4</sup>(DMSO)] (**4**): To the refluxing solution of ligand H<sub>2</sub>L<sup>4</sup> (1 mmol) in 30 mL ethanol, MoO<sub>2</sub>(acac)<sub>2</sub> (1 mmol) was added. The color of the solution immediately turned red. After 3 h of reflux, the solution was cooled, filtered. The dark brown residue obtained was crystallized in DMSO. Slow evaporation of the solution for 2 days produced orange crystals suitable for X-Ray analysis. Yield: 0.29 g (52 %). Anal. Calcd for C<sub>24</sub>H<sub>20</sub>MoN<sub>2</sub>O<sub>6</sub>S: C, 51.43; H, 3.60; N, 5.00; S, 5.72. Found: C, 51.40; H, 3.62; N, 5.04; S, 5.70 %. FTIR (KBr,  $\nu_{\max}/\text{cm}^{-1}$ ):  $\nu(\text{O-H})$  3440,  $\nu(\text{C=N})$  1587,  $\nu(\text{M=O})$  937, 917. UV-Vis (DMSO):  $\lambda_{\max}$ , nm ( $\epsilon$ ,  $\text{dm}^3 \text{mol}^{-1} \text{cm}^{-1}$ ): 428 (1193), 403 (980), 341 (2300), 260 (4580). <sup>1</sup>H NMR (400 MHz, DMSO-d<sub>6</sub>):  $\delta$  (ppm) = 11.29 (s, 1H, -OH), 10.15 (s, 1H, -CH), 8.64–7.24 (m, 12H, aromatic), 2.50 (s, 6H, DMSO). <sup>13</sup>C NMR (100 MHz, DMSO-d<sub>6</sub>):  $\delta$  (ppm) = 168.23, 160.87, 154.70, 153.95, 151.23, 147.35, 136.89, 133.05, 131.37, 121.49, 129.38, 129.13, 129.05, 127.44, 126.38, 125.45, 124.22, 122.37, 120.75, 116.14, 112.14, 111.46, 40.83. ESI-MS:  $m/z$  560.15 [M]<sup>+</sup>.

[MoO<sub>2</sub>L<sup>5</sup>(EtOH)] (**5**): To the refluxing solution of ligand H<sub>2</sub>L<sup>5</sup> (1 mmol) in 30 mL ethanol, MoO<sub>2</sub>(acac)<sub>2</sub> (1 mmol) was added. The color of the solution immediately turned red. After 3 h of reflux, the solution was cooled, filtered. Dark yellow crystals were obtained on slow evaporation of the filtrate after two days. Slow evaporation of the solution for 2 days produced orange crystals suitable for X-Ray analysis. Yield: 0.26 g (53 %). Anal. Calcd for C<sub>21</sub>H<sub>20</sub>MoN<sub>2</sub>O<sub>6</sub>: C, 51.23; H, 4.09; N, 5.69. Found: C, 51.21; H, 3.60; N, 5.65 %. FTIR (KBr,  $\nu_{\max}/\text{cm}^{-1}$ ):  $\nu(\text{O-H})$  3310,  $\nu(\text{C=N})$  1594,  $\nu(\text{M=O})$  917, 902. UV-Vis (DMSO):  $\lambda_{\max}$ , nm ( $\epsilon$ ,  $\text{dm}^3 \text{mol}^{-1} \text{cm}^{-1}$ ): 395 (6293), 327 (17846), 268 (18160). <sup>1</sup>H NMR (400 MHz, DMSO-d<sub>6</sub>):  $\delta$  (ppm) = 11.44 (s, 1H, -OH), 8.57–7.00 (m, 10H, aromatic), 4.35 (1H, OH, ethanol), 3.45 (q, 2H, -CH<sub>2</sub> ethanolic), 3.43 (s, 3H, -CH<sub>3</sub>), 1.06 (t, 3H, -CH<sub>3</sub> ethanolic). <sup>13</sup>C NMR (100 MHz, DMSO-d<sub>6</sub>):  $\delta$  (ppm) = 163.55, 157.65, 136.62, 132.84, 132.17, 129.78, 129.66, 129.59, 129.39,

129.08, 128.55, 127.17, 126.99, 126.30, 125.60, 124.34, 124.17, 117.02, 103.93, 12.10. ESI-MS:  $m/z$  492.02  $[M]^+$ .

$[\text{MoO}_2\text{L}^6(\text{DMSO})]$  (**6**): To the refluxing solution of ligand  $\text{H}_2\text{L}^6$  (1 mmol) in 30 mL ethanol,  $\text{MoO}_2(\text{acac})_2$  (1 mmol) was added. The color of the solution immediately turned red. After 3 h of reflux, the solution was cooled, filtered. The dark brown residue obtained was crystallized in DMSO. Slow evaporation of the solution for 2 days produced orange crystals suitable for X-Ray analysis. Yield: 0.27 g (48 %). Anal. Calcd for  $\text{C}_{22}\text{H}_{22}\text{MoN}_2\text{O}_7\text{S}$ : C, 47.66; H, 4.00; N, 5.05; S, 5.78. Found: C, 47.61; H, 4.05; N, 5.00; S, 5.76 %. FTIR (KBr,  $\nu_{\text{max}}/\text{cm}^{-1}$ ):  $\nu(\text{O-H})$  3454,  $\nu(\text{C=N})$  1614,  $\nu(\text{M=O})$  926, 904. UV-Vis (DMSO):  $\lambda_{\text{max}}$ , nm ( $\epsilon$ ,  $\text{dm}^3 \text{mol}^{-1} \text{cm}^{-1}$ ): 400 (1106), 332 (2346), 259 (3320).  $^1\text{H}$  NMR (400 MHz,  $\text{DMSO-d}_6$ ):  $\delta$  (ppm) = 11.47 (s, 1H,  $-\text{OH}$ ), 8.52–6.58 (m, 9H, aromatic), 3.84 (s, 3H,  $-\text{OCH}_3$ ), 2.77 (s, 3H,  $-\text{CH}_3$ ), 2.50 (s, 6H, DMSO).  $^{13}\text{C}$  NMR (100 MHz,  $\text{DMSO-d}_6$ ):  $\delta$  (ppm) = 167.19, 164.77, 164.15, 157.56, 154.71, 136.78, 133.17, 131.22, 129.46, 129.12, 127.44, 126.39, 124.28, 116.46, 115.94, 111.13, 110.17, 103.40, 56.29, 47.39, 17.64. ESI-MS:  $m/z$  554.02  $[M]^+$ .

$[\text{MoO}_2\text{L}^7(\text{DMSO})]$  (**7**): To the refluxing solution of ligand  $\text{H}_2\text{L}^7$  (1 mmol) in 30 mL ethanol,  $\text{MoO}_2(\text{acac})_2$  (1 mmol) was added. The color of the solution immediately turned red. After 3 h of reflux, the solution was cooled, filtered. The dark brown residue obtained was crystallized in DMSO. Red microcrystalline residue was obtained. Yield: 0.28 g (52 %). Anal. Calcd for  $\text{C}_{21}\text{H}_{20}\text{MoN}_2\text{O}_7\text{S}$ : C, 46.67; H, 3.73; N, 5.18; S, 5.93. Found: C, 46.61; H, 3.70; N, 5.14; S, 5.90 %. FTIR (KBr,  $\nu_{\text{max}}/\text{cm}^{-1}$ ):  $\nu(\text{O-H})$  3491,  $\nu(\text{C=N})$  1615,  $\nu(\text{M=O})$  966, 942. UV-Vis (DMSO):  $\lambda_{\text{max}}$ , nm ( $\epsilon$ ,  $\text{dm}^3 \text{mol}^{-1} \text{cm}^{-1}$ ): 402 (3177), 334 (10326), 261 (12206).  $^1\text{H}$  NMR (400 MHz,  $\text{DMSO-d}_6$ ):  $\delta$  (ppm) = 11.26 (s, 1H,  $-\text{OH}$ ), 9.10 (s, 1H,  $-\text{CH}$ ), 8.53–5.74 (m, 9H, aromatic), 3.79 (s, 3H,  $-\text{OCH}_3$ ), 2.50 (s, 6H, DMSO).  $^{13}\text{C}$  NMR (100

MHz, DMSO- $d_6$ ):  $\delta$  (ppm) = 169.38, 157.02, 154.61, 154.19, 136.93, 131.54, 129.49, 129.22, 127.43, 126.39, 124.31, 122.61, 120.56, 119.92, 117.38, 116.20, 111.55, 111.33, 56.19, 40.78. ESI-MS:  $m/z$  540.85 [M]<sup>+</sup>.

## 2.4. Crystallography

### 2.4.1. General handling and description of equipment

Appropriate single-crystals were selected under a polarization microscope. Inherent impurities of other crystals were removed carefully and appropriate size was achieved by cutting. Therefore, crystal shape and size given in the table of crystallographic data only approximate the properties of the crystal measured but do not reflect habit and size of the naturally grown crystals. Crystals of **1** was mounted on a 100  $\mu\text{m}$  round LithoLoop (Molecular Dimensions) using Paratone N (Hampton Research) while those of **2–6** were mounted on a 50  $\mu\text{m}$  MicroMesh MiTeGen Micromount<sup>TM</sup> using FROMBLIN Y perfluoropolyether (LVAC 16/6, Aldrich) before they were centred on a Bruker Kappa APEX II CCD-based 4-circle X-ray diffractometer using graphite monochromated Mo  $K_\alpha$  radiation ( $\lambda = 0.71073 \text{ \AA}$ ) of a fine focus molybdenum-target X-ray tube operating at 50 kV and 30 mA. Crystal cooling was achieved with Cobra, the non-liquid nitrogen Cryostream device (Oxford Cryosystems) in case of **1** and a Kryoflex low temperature device in case of **2–6**, respectively.

### 2.4.2. Data collection and handling

In case of **1** data collection strategy analysis as well as diffraction data processing were performed automatically with *CrysAlisPro* (data collection, cell refinement and data reduction). Initial unit cell parameters of **2–6** were obtained by least-squares refinement of the xyz centroids of strong to medium strong reflections harvested from a series of 12 frames in each of three orthogonally related regions of the reciprocal space using the *evaluate* routine

of the APEX software suite [95]. Final unit cell parameters were calculated at the end of intensity measurements from xyz centroids of up to 10000 well-centred intense reflections of the complete data set. Intensity data were collected via  $\omega$ - and  $\varphi$ -scans in a range up to  $2\Theta = 56^\circ$  with scan widths of  $0.5^\circ$  and scan speeds of 3 - 10 s/frame at a crystal to detector distance of 40 mm. Collecting strategies were optimized by use of the *collect* routine of the APEX software suite in order to reach an average data redundancy of 10 or better in about 24 h. Information about crystal mosaicity as well as its scattering behaviour at higher  $\Theta$  values was derived from prescans for unit cell determinations. Integrated intensities were obtained with the Bruker SAINT [96] software package using a narrow-frame algorithm performing spatial corrections of frames, background subtractions, Lorentz and polarization corrections, profile fittings and error analyses. Semi-empirical absorption corrections based on equivalent reflections were made by use of the program SADABS [97]. Details on the data collection parameters applied on the individual crystals are summarized in **Table 1** with  $R_{\text{int}} = \Sigma|F_o^2 - F_o^2(\text{mean})|/\Sigma[F_o^2]$  and  $R_{\text{sigma}} = \Sigma[\sigma(F_o^2)]/\Sigma[F_o^2]$

Space groups [98] were determined from systematic absences and E-value statistics evaluated by the *examine data* routine of the APEX program suite.

#### 2.4.3. General information on structure solution and refinement

Structures were solved by direct methods and subsequent difference Fourier syntheses of the program SHELXS [99] and refined by full-matrix least-squares techniques on  $F^2$  with SHELXL [99], applying anisotropic displacement factors for all non-hydrogen atoms. Atomic scattering factors were taken from International Tables for Crystallography [100].

Final agreement indices were defined as following:  $R_1 = \Sigma||F_o| - |F_c||/\Sigma|F_o|$  and  $wR_2 = [\Sigma[w(F_o^2 - F_c^2)^2]/\Sigma(F_o^2)^2]^{1/2}$ . Weighting function used:  $w = 1/[\sigma^2(F_o^2) + (pP)^2 + qP]$  with  $P = (F_o^2 + 2F_c^2)/3$ .  $\text{Goof} = [\Sigma[w(F_o^2 - F_c^2)^2]/(n-p)]^{1/2}$  where  $n$  is the number of reflections and  $p$  is the total number of parameters refined. All non-hydrogen atoms were refined with

anisotropic displacement parameters and hydrogen atoms with common isotropic displacement parameters for chemically related groups of hydrogen atoms.

Although most of the hydrogen atoms could be localised in difference Fourier syntheses, those of the organic groups were refined in geometrically optimized positions riding on the corresponding carbon atoms with C-H distances of 0.98 Å (-CH<sub>3</sub>), 0.99 Å (-CH<sub>2</sub>-) 1.00 Å (-CH=) and 0.95 Å (CH<sub>arom</sub>). Hydrogen atoms bonded to oxygen were refined with respect to a common O-H distance of 0.96 Å before they were fixed and allowed to ride on the corresponding oxygen atoms. Further details on the results of structure refinement are summarized in **Table 1**.

Disorder only was observed in case of the ethanol molecule of **5** as a whole with site occupancies of 0.816/0.184. Bond lengths between the carbon atoms as well as between carbon and oxygen were refined with bond constrains while the anisotropic displacement parameters were set equal for neighbouring atoms.

Figures were drawn using DIAMOND [101] and Mercury [102], respectively. In the ball-and-stick models, all atoms are drawn as thermal displacement ellipsoids of the 40% level with exception of the hydrogen atoms which are shown as spheres of arbitrary radii. Hydrogen bonds are drawn in red as dashed sticks.

Table 1 Crystal data and structure refinement

Complex	1	2	3	4	5	6
Empirical formula	C <sub>22</sub> H <sub>24</sub> MoN <sub>2</sub> O <sub>7</sub>	C <sub>21</sub> H <sub>20</sub> MoN <sub>2</sub> O <sub>7</sub> S	C <sub>20</sub> H <sub>17</sub> BrMoN <sub>2</sub> O <sub>6</sub> S	C <sub>24</sub> H <sub>20</sub> MoN <sub>2</sub> O <sub>6</sub> S	C <sub>21</sub> H <sub>20</sub> MoN <sub>2</sub> O <sub>6</sub>	C <sub>22</sub> H <sub>22</sub> MoN <sub>2</sub> O <sub>7</sub> S
Formula weight	524.37	540.39	589.27	560.42	492.33	554.42
Temperature	100(2) K	100(2) K	100(2) K	100(2) K	200(2) K	100(2) K
Wavelength [Å]	1.54184	0.71073	0.71073	0.71073	0.71073	0.71073
Crystal system, space group	Monoclinic, P2 <sub>1</sub> /n	Monoclinic, P2 <sub>1</sub> /c	Triclinic, P $\bar{1}$	Triclinic, P $\bar{1}$	Monoclinic, P2 <sub>1</sub> /c	Monoclinic, P2 <sub>1</sub> /c
Unit cell dimensions						
a [Å]	16.3339(3)	10.8937(3)	8.9569(4)	8.1458(5)	7.9829(3)	7.9379(4)
b [Å]	7.9180(1)	12.3965(3)	10.9615(5)	11.7962(6)	15.7158(8)	11.8274(5)
c [Å]	18.8705(4)	15.7762(6)	11.7760(5)	12.3553(6)	16.5012(8)	23.9551(8)
$\alpha$ [°]	90	90	91.519(2)	98.979(2)	90	90
$\beta$ [°]	115.598(3)	101.033(2)	108.090(2)	102.085(2)	100.169(2)	96.283(2)
$\gamma$ [°]	90	90	111.060(2)	105.001(1)	90	90
Volume [Å <sup>3</sup> ]	2201.01(8)	2091.10(11)	1013.12(8)	1093.20(10)	2037.68(16)	2235.51(16)
Z, Z', Calculated density [g/cm <sup>3</sup> ]	4, 1, 1.582	4, 1, 1.716	2, 1, 1.932	2, 1, 1.703	4, 1, 1.605	4, 1, 1.647
Absorption coefficient [mm <sup>-1</sup> ]	5,283	0.775	2,765	0.742	0.685	0.727
F(000)	1072	1096	584	568	1000	1128
Crystal size [mm]	0.1 x 0.08 x 0.05	0.15 x 0.10 x 0.06	0.34 x 0.23 x 0.06	0.35 x 0.25 x 0.22	0.49 x 0.20 x 0.13	0.27 x 0.22 x 0.07
Theta range for data collection [°]	3.002 to 74.014	2.63 to 28.00	3.50 to 28.00	2.79 to 28.00	2.59 to 28.00	2.94 to 28.00
Reflections collected	21232	50824	78032	65582	68347	71048
Reflections unique, R <sub>int</sub>	4397, 0.0166	5044, 0.0965	4887, 0.0517	5280, 0.0675	4863, 0.0767	5295, 0.0594
Completeness to theta = 67.684	99.9%	99.9%	99.8%	99.8%	98.7%	98.0%
Max./min. transmission	0.803/0.59479	0.9521/0.8919	0.8429/0.4577	0.8514/0.7829	0.9150/0.7293	0.9536/0.8256
Data / restraints / parameters	4397 / 0 / 300	5044 / 0 / 295	4887 / 0 / 286	5280 / 0 / 313	4863 / 4 / 286	5295 / 0 / 307
Goodness-of-fit on F <sup>2</sup>	1,078	0.868	1,075	1,097	1,096	1,143
R <sub>1</sub> , wR <sub>2</sub>	0.0239, 0.0636	0.0449, 0.0834	0.0265, 0.0655	0.0225, 0.0589	0.0314, 0.0811	0.0433, 0.0949
R <sub>1</sub> , wR <sub>2</sub>	0.0239, 0.0637	0.0738, 0.0917	0.0315, 0.0683	0.0238, 0.0595	0.0393, 0.0889	0.0562, 0.0996
Extinction coefficient	n/a	0.0031(3)	0.0064(6)	0.0048 (6)	n/a	0.0011 (2)
Largest diff. peak / hole e.Å <sup>-3</sup>	0.360/-0.799	0.839/-0.741	0.571/-0.483	0.573/-0.564	0.715/-0.913	0.743/-0.863
CCDC-number	1528262	1543188	1543189	1543190	1543191	1543192

## 2.5 Catalytic reactions

### 2.5.1. Oxidation of benzoin

For this oxidation reaction, benzoin (1.06 g, 5 mmol), aqueous 30% H<sub>2</sub>O<sub>2</sub> (1.71 g, 15 mmol) and catalyst (0.0005 g) were taken in 10 mL of methanol. The reaction was carried out at refluxing temperature for 4 h. The progress of the reaction was examined by withdrawing small aliquots at different time intervals and samples were extracted with n-hexane and then analysing them quantitatively by gas chromatography. The effect of various parameters such as amount of catalyst, amount of oxidant, and solvent were studied to optimize the reaction conditions.

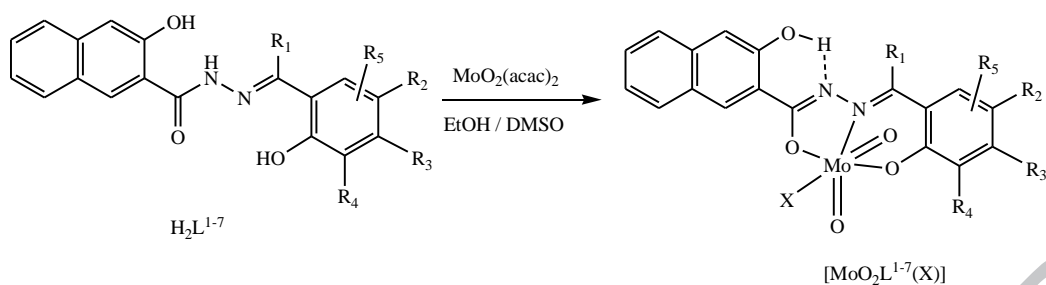
### 2.5.2. Oxidative bromination of salicylaldehyde

Dioxidomolybdenum complexes are also checked towards oxidative bromination of salicylaldehyde. In a typical reaction, salicylaldehyde (0.610 g, 5 mmol) was added to an aqueous solution (20 mL) of KBr (1.785 g, 15 mmol), followed by addition of aqueous 30% H<sub>2</sub>O<sub>2</sub> (1.71 g, 15 mmol). The catalyst (0.0010 g) and 70% HClO<sub>4</sub> (0.536 g, 3.75 mmol) were added, and the reaction mixture was stirred at room temperature. Three additional 3.75 mmol portions of 70% HClO<sub>4</sub> were further added to the reaction mixture in three equal portions in 30 minutes intervals under continuous stirring. After 2 h, the white products have separated out which was extracted with CH<sub>2</sub>Cl<sub>2</sub> and dried. The crude mass was dissolved in methanol and this material was subjected to gas chromatography, and the identity of the products confirmed by GC-MS.

### 3. Results and Discussion

#### 3.1. Synthesis

In the present study, seven dioxidomolybdenum(VI) complexes have been prepared from various aroylazine ligands containing a bulky 3-hydroxy-2-naphthoic substituent (**Scheme 1**) in order to observe their influence, if any, on the catalytic properties of the complexes. Reaction of the aroylazines with  $\text{MoO}_2(\text{acac})_2$  in ethanol yielded orange or yellow crystalline residue in good yield. Single crystals of **1** and **5** were obtained directly from the slow evaporation of the filtrate of the reaction mixture, while complexes **2–4** and **6** were obtained by recrystallizing the residue obtained in DMSO. Complexes (**1–7**) were completely soluble in DMF, DMSO and partially soluble in  $\text{CH}_3\text{CN}$ , ethanol and methanol. Magnetic susceptibility and molar conductivity data indicate that all the complexes (**1–7**) are diamagnetic and electrically non-conducting in solution. The detailed characterization of all the complexes has been discussed in the respective section (IR, UV-Vis, NMR, ESI-MS and X-Ray crystallography).



R <sub>1</sub>	R <sub>2</sub>	R <sub>3</sub>	R <sub>4</sub>	R <sub>5</sub>	Ligand	X	Complex
H	H	H	H	-	H <sub>2</sub> L <sup>1</sup>	EtOH	[MoO <sub>2</sub> L <sup>1</sup> (EtOH)].EtOH (1)
H	H	H	OCH <sub>3</sub>	-	H <sub>2</sub> L <sup>2</sup>	DMSO	[MoO <sub>2</sub> L <sup>2</sup> (DMSO)] (2)
H	Br	H	H	-	H <sub>2</sub> L <sup>3</sup>	DMSO	[MoO <sub>2</sub> L <sup>3</sup> (DMSO)] (3)
H	H	H	H	Ph	H <sub>2</sub> L <sup>4</sup>	DMSO	[MoO <sub>2</sub> L <sup>4</sup> (DMSO)] (4)
CH <sub>3</sub>	H	H	H	-	H <sub>2</sub> L <sup>5</sup>	EtOH	[MoO <sub>2</sub> L <sup>5</sup> (EtOH)] (5)
CH <sub>3</sub>	H	OCH <sub>3</sub>	H	-	H <sub>2</sub> L <sup>6</sup>	DMSO	[MoO <sub>2</sub> L <sup>6</sup> (DMSO)] (6)
H	OCH <sub>3</sub>	H	H	-	H <sub>2</sub> L <sup>7</sup>	DMSO	[MoO <sub>2</sub> L <sup>7</sup> (DMSO)] (7)

**Scheme 1.** Synthesis of the dioxidomolybdenum(VI) complexes [MoO<sub>2</sub>L<sup>1</sup>(X)].X (1) and [MoO<sub>2</sub>L<sup>2-7</sup>(X)] (2–7).

### 3.2. Spectral Characteristics

Spectral characteristics of all the ligands (H<sub>2</sub>L<sup>1-7</sup>) and complexes (1–7) are given in the *Experimental Section*. All the ligands exhibit two bands in the range of 3387–3556 cm<sup>-1</sup> in the FTIR spectra due to the presence of two –OH groups [32,103,104]. The stretching for the –NH group is found the region between 3003–3008 cm<sup>-1</sup> and the –C=O stretching frequency is obtained in the range of 1642–1649 cm<sup>-1</sup> [32,103,104]. The disappearance of –NH, –C=O and one of the –OH stretching bands in the IR spectra of the complexes indicate the formation of metal complexes. The sharp peak at 1587–1615 cm<sup>-1</sup> is probably due to the –C=N–N=C– moiety in the complex formed [32,103,104]. The presence of two strong peaks in the range 902–966 cm<sup>-1</sup> is due to the Mo=O stretching [32,103,104] which indicates the presence of dioxido group in the complexes.

Electronic spectra of the complexes were recorded in DMSO. All the complexes exhibit medium intensity bands in the range 382–428 nm assignable to ligand to metal charge transfer (LMCT) and strong intensity bands within 259–341 nm which may be due to ligand centered transitions [32,103,104]. The representative absorbance spectrum of **6** is given in **Fig. 1**.

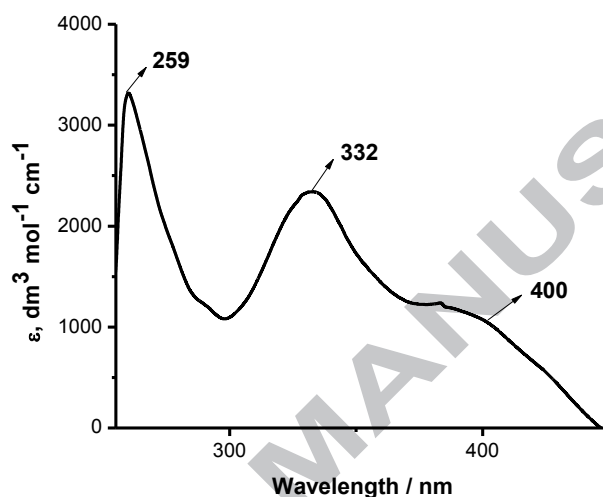


**Fig. 1.** Electronic absorption spectrum of **6** ( $1.5 \times 10^{-4}$  M) in DMSO.

$^1\text{H}$  and  $^{13}\text{C}$  NMR of all the compounds were recorded in  $\text{DMSO-}d_6$  and the data are given in the experimental section. The coordinating modes of  $\text{H}_2\text{L}^{1-7}$  were confirmed by comparing their  $^1\text{H}$  NMR spectral patterns with those of the corresponding complexes. The  $^1\text{H}$  NMR spectra of all the ligands ( $\text{H}_2\text{L}^{1-7}$ ) and complexes (**1–7**) are given in **Figs. S1–S14**. The  $^1\text{H}$  NMR spectrum of the free ligands exhibits resonance in the range  $\delta = 13.55\text{--}11.94$  ppm due to  $\text{--NH}$  group [32,103,104]. Two peaks in the range of  $\delta = 12.25\text{--}10.92$  ppm were observed due phenolic  $\text{--OH}$  groups, while the singlet at  $\delta = 9.57\text{--}8.21$  ppm was due to the azomethine  $\text{--CH}$  proton [32,103,104]. The aromatic protons from ligands are clearly observed in the expected region  $\delta = 8.53\text{--}6.49$  ppm. Singlets for the  $\text{--OCH}_3$  protons of  $\text{H}_2\text{L}^2$ ,  $\text{H}_2\text{L}^6$  and  $\text{H}_2\text{L}^7$  were observed at around 3.78 ppm, while singlets for the  $\text{--CH}_3$  protons of  $\text{H}_2\text{L}^5$  and  $\text{H}_2\text{L}^6$  were observed at 3.36 and 2.43 ppm respectively. In the NMR spectra of complexes, one of the peak for the aromatic  $\text{--OH}$  proton disappeared due to the deprotonation of phenolic

group. The aromatic protons of the complexes were observed in the range  $\delta = 8.64\text{--}6.58$  ppm. In the  $^{13}\text{C}$  NMR spectra of the ligands  $\text{H}_2\text{L}^{1-5}$ , spectral signals for the aromatic carbons are found in the downfield region in the range  $\delta = 169.95\text{--}102.06$  ppm [32,103,104]. The signals for the aliphatic carbons of for  $-\text{OCH}_3$  and  $-\text{CH}_3$  of  $\text{H}_2\text{L}^2$ ,  $\text{H}_2\text{L}^5$ ,  $\text{H}_2\text{L}^6$  and  $\text{H}_2\text{L}^7$  appeared in the range of  $\delta = 55.93\text{--}13.60$  ppm. While in the  $^{13}\text{C}$  NMR spectra of complexes **1–7**, signals for the aromatic carbons are found in the downfield region in the range  $\delta = 169.65\text{--}111.42$  ppm [32,103,104]. The  $^{13}\text{C}$  NMR spectra of all the ligands ( $\text{H}_2\text{L}^{1-7}$ ) and complexes (**1–7**) are given in **Figs. S15–S28**.

### 3.3. ESI-MS

ESI-MS spectra of **1–7** have been recorded in  $\text{CH}_3\text{CN}$ . The characteristic molecular ion peak for **1–7** appear at  $524.20 [\text{M}]^+$ ,  $540.21 [\text{M}]^+$ ,  $589.50 [\text{M}]^+$ ,  $560.15 [\text{M}]^+$ ,  $492.02[\text{M}]^+$ ,  $554.02 [\text{M}]^+$ , and  $540.85 [\text{M}]^+$ . The representative ESI-MS of **7** is given in **Fig. S29**.

### 3.4. Electrochemical properties

Electrochemical properties of the complexes have been studied by cyclic voltammetry in  $\text{CH}_3\text{CN}$  solution (0.1 M TBAP). Voltammetric data are given in **Table 2** and a representative voltammogram of **6** is given in **Fig. 2**. The CV traces of all the complexes are similar and exhibit two irreversible reductive responses within the potential window  $-0.50$  to  $-1.36$  V, which are assigned to  $\text{Mo}^{\text{VI}}/\text{Mo}^{\text{V}}$  and  $\text{Mo}^{\text{V}}/\text{Mo}^{\text{IV}}$  processes respectively [89]. Two oxidation waves at positive potentials in the range of  $+1.25$  to  $+1.69$  V are assigned to the oxidation of the coordinated ligand [105]. The representative cyclic voltammogram of **6** showing the oxidation potentials is given in **Fig. S30**. Single electron processes were verified by comparing the current height with that of the standard ferrocene–ferrocenium couple under identical experimental conditions.

**Table 2** Cyclic voltammetric results for oxidomolybdenum(VI) complexes (**1** – **7**) at 298 K

Complexes	$E_{pc}$ [V] <sup>[a]</sup>
<b>1</b>	-0.51, -1.34
<b>2</b>	-0.54, -1.30
<b>3</b>	-0.50, -1.31
<b>4</b>	-0.52, -1.35
<b>5</b>	-0.52, -1.36
<b>6</b>	-0.51, -1.32
<b>7</b>	-0.55, -1.36

<sup>[a]</sup>Solvent: CH<sub>3</sub>CN; working electrode: platinum; auxiliary electrode: platinum; reference electrode: Ag/AgCl; supporting electrolyte: 0.1 M TBAP; scan rate: 50 mV/s.  $E_{pc}$  is the cathodic peak potential.

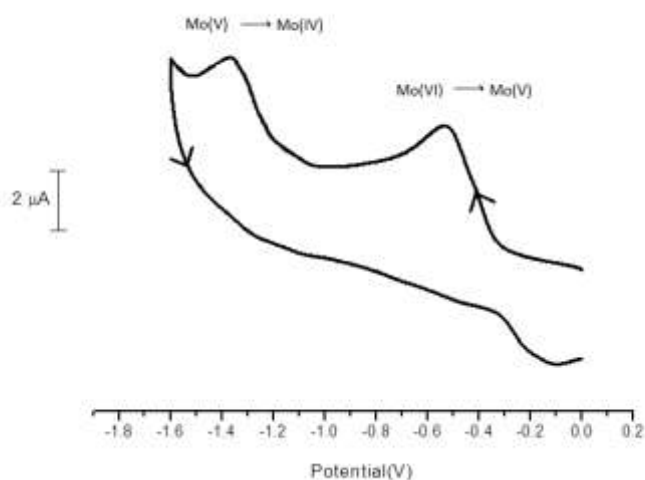


**Fig. 2.** Cyclic voltammogram of **6** in CH<sub>3</sub>CN; scan rate: 50 mV/s and potentials recorded vs Ag/AgCl.

## 3.5. X-ray structure description

The solid state structures of complexes **1–6** are shown in **Fig. 3** and the selected bond lengths and bond angles are listed in **Table 3**.

**Table 3** Selected bond lengths [Å] and angles (°) for complexes **1–6**

Complexes	1	2	3	4	5	6
<i>Bond lengths</i>						
O(1)-C(1)	1.319(2)	1.322(4)	1.319(2)	1.326(2)	1.310(2)	1.309(4)
O(2)-C(12)	1.350(2)	1.365(3)	1.345(3)	1.341(2)	1.351(3)	1.351(4)
Mo(1)-N(1)	2.236(1)	2.240(3)	2.256(2)	2.227(1)	2.261(2)	2.253(3)
Mo(1)-O(3)	1.690(1)	1.694(2)	1.698(2)	1.701(1)	1.683(2)	1.698(2)
Mo(1)-O(4)	1.718(1)	1.718(2)	1.700(2)	1.713(1)	1.698(2)	1.695(2)
Mo(1)-O(2)	1.925(1)	1.919(2)	1.928(2)	1.934(1)	1.908(2)	1.922(2)
Mo(1)-O(1)	2.007(1)	2.036(2)	1.996(2)	2.012(1)	2.018(2)	2.009(2)
Mo(1)-N(1)	2.236(1)	2.240(3)	2.256(2)	2.227(1)	2.261(2)	2.253(3)
Mo(1)-O(solvent)	2.292(1)	2.347(2)	2.309(2)	2.322(1)	2.329(4)	2.270(2)
<i>Bond angles</i>						
O(3)-Mo(1)-O(4)	105.45(6)	105.7(1)	105.58(8)	105.59(6)	105.29(9)	105.0(1)
O(3)-Mo(1)-O(2)	99.26(6)	99.5(1)	99.46(7)	100.11(5)	99.90(9)	100.2(1)
O(4)-Mo(1)-O(2)	103.54(6)	104.0(1)	103.01(7)	102.49(5)	103.14(9)	103.5(1)
O(3)-Mo(1)-O(1)	97.98(6)	95.0(1)	96.17(7)	96.95(5)	97.91(9)	96.6(1)
O(4)-Mo(1)-O(1)	96.67(5)	96.5(1)	96.78(7)	97.94(5)	97.20(8)	97.1(1)
O(2)-Mo(1)-O(1)	148.75(5)	150.5(1)	150.36(6)	148.66(5)	148.21(7)	149.0(1)
O(3)-Mo(1)-N(1)	93.81(6)	94.3(1)	93.55(7)	94.11(5)	95.40(8)	90.7(1)
O(4)-Mo(1)-N(1)	158.99(6)	158.0(1)	158.93(7)	159.20(5)	158.13(8)	162.4(1)
O(2)-Mo(1)-N(1)	81.07(5)	81.3(1)	82.00(6)	80.06(5)	79.72(7)	81.1(1)
O(1)-Mo(1)-N(1)	71.94(5)	72.1(1)	71.99(6)	72.62(4)	72.57(6)	72.76(1)
O(3)-Mo(1)- O(solvent)	169.66(6)	167.8(1)	167.42(7)	169.83(5)	172.80(9)	166.7(1)

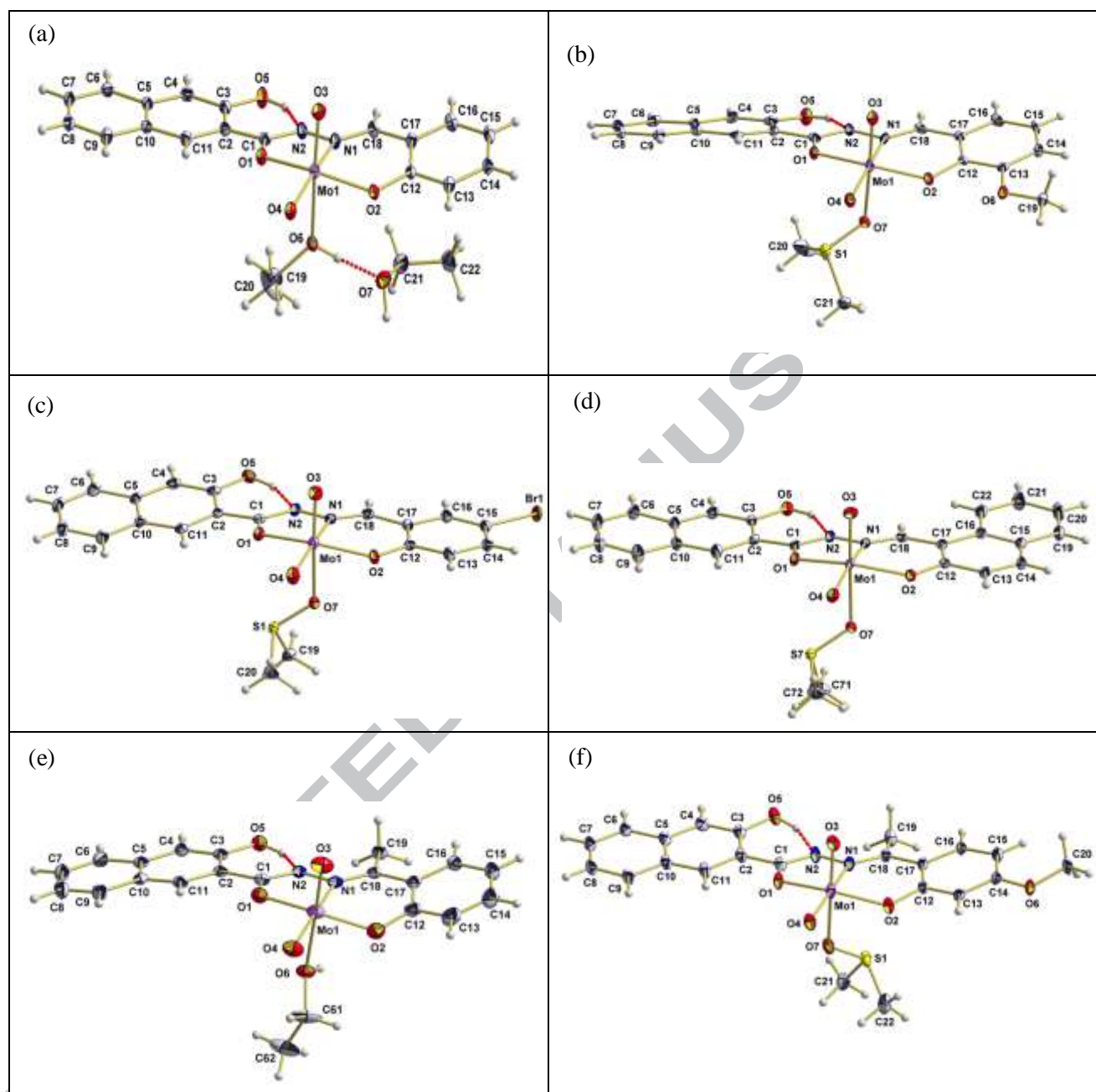


**Fig. 3.** Ball-and-stick models of complexes with the atomic numbering scheme used [Fig. 3(a): 1; Fig. 3(b): 2; Fig. 3(c): 3; Fig. 3(d): 4; Fig. 3(e): 5; Fig. 3(f): 6] with exception of the hydrogen atoms, which are drawn as spheres of arbitrary radius, all other atoms are represented as thermal displacement ellipsoids of 50% probability level.

The asymmetric unit of all these complexes consists of a complete formula unit. All complexes exhibit the same structural features consisting of a central molybdenum atom coordinated by two double bonded oxygen atoms, the tridentate organic ligand and an additional solvent molecule like dimethyl sulfoxide (**2**, **3**, **4**, **6**) or ethanol (**1**, **5**) acting as Lewis Base. In case of **1**, a second ethanol molecule is hydrogen bonded to the ethanol molecule coordinating the Mo atom. Conformational differences within the complexes arise from steric and electronic requirements of the individual ligands. At the metal site, the MoO<sub>2</sub>-fragment with its double bonded oxygen atoms is only slightly affected by ligand effects. The Mo=O bonds are in a very narrow range [1.690(1) – 1.718(2) Å, mean value: 1.701(11) Å] as are the O=Mo=O bond angles [105.0(1)°-105.7(1)°, mean value: 105.4(3)°]. In each case, the organic ligand coordinates the Mo atom via two oxygen atoms and one nitrogen atom. Significant bond length variations are observed in case of the corresponding Mo-O bonds. Mo-O bonds of the carbonyl group [O(1)] are slightly weaker [1.996(2) – 2.036(2) Å, mean value: 2.013(13) Å] as those [1.908(2) -1.934(1) Å, mean value: 1.923(9) Å] of the alkoxide group [O(2)]. Conversely, the corresponding C-O bonds of the carbonyl group are shorter [1.309(4) – 1.326(2) Å, mean value: 1.318(7) Å] as those of the alkoxide group [1.345(3) – 1.365(3) Å, mean value: 1.351(8) Å]. Both types of coordinative Mo-O bonds are shorter than the coordinative Mo-N bonds [N(1), 2.227(3) – 2.261(3) Å, mean value 2.246(13) Å]. As a result of the ligand coordination to the Mo atom a 5-membered, and a six-membered chelate ring are formed. In all compounds, the oxygen atom of the solvent molecule (DMSO, EtOH) acting as Lewis Base to the central Mo atom gives rise to the weakest bond [2.270(2) - 2.347(2) Å, mean value: 2.312(28) Å] in the complex. Lability of this bond is expressed by the broad range these Mo-O bond cover, as well as by the relatively large bond angles [166.7(1)° – 172.80(9)°, mean value 169.0(22)°] between the solvent O atoms and their *trans* positioned, double bonded O(3) atoms.

An additional common feature of all compounds is the presence of an intramolecular hydrogen bond between the OH group [O(5)-H(5)] at C(3) and the non-coordinating nitrogen atom [N(2)], giving rise to a six-membered, nearly planar ring (**Fig. 4**). These hydrogen bonds are characterized by O...N distances and O-H...N angles of 2.538(2) – 2.630(2) Å, and 145.6° - 153.8°, respectively.

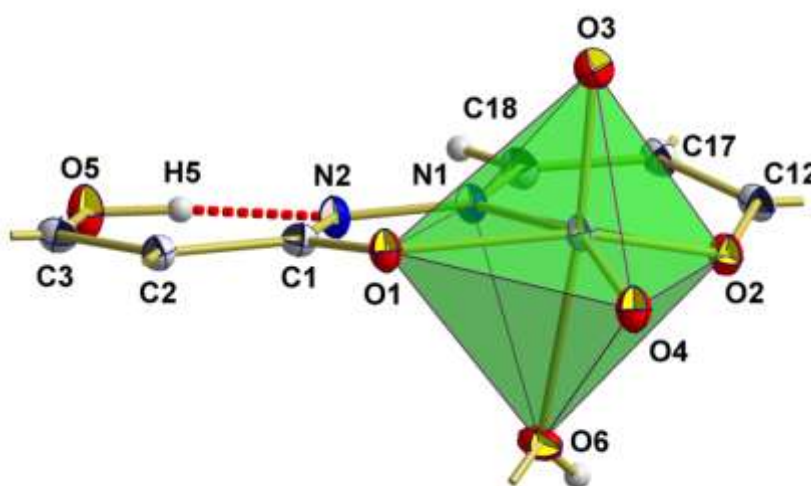
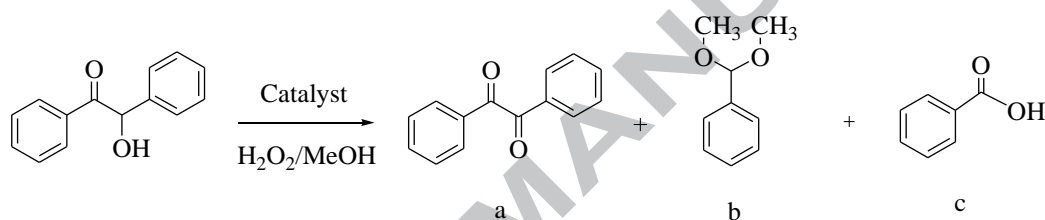


**Fig. 4.** View on the coordination sphere of the Mo atom and intramolecular O-H...N hydrogen bond. With exception of the hydrogen atoms, which are drawn as spheres of arbitrary radius, all other atoms are represented as thermal displacement ellipsoids of 50% probability level. For clarity, only the backbone of these structural features is drawn.

### 3.6. Catalytic activity studies

#### 3.6.1. Oxidation of benzoin

The oxidation of benzoin is one of the most significant organic transformations in chemistry. Benzil, one of the oxidized products of benzoin, is a very functional intermediate for the synthesis of heterocyclic compounds and benzylic acid rearrangements [106]. The molybdenum complexes successfully catalyze the oxidation of benzoin using 30% aqueous  $\text{H}_2\text{O}_2$  as an oxidant. **Scheme 2** shows the main products obtained from this reaction.



**Scheme 2.** Various oxidation products of benzoin. (a) benzil, (b) benzaldehyde-dimethyl acetal and (c) benzoic acid.

$[\text{MoO}_2\text{L}^1(\text{EtOH})]\cdot\text{EtOH}$  (**1**) was considered as a representative catalyst to optimize the reaction conditions for the maximum oxidation of benzoin. The effect of oxidant was studied by considering the oxidant to substrate ratios of 1 : 1, 2 : 1 and 3 : 1 for the fixed amount of catalyst (0.0010 g) and substrate (1.06 g, 5 mmol) in 10 mL of refluxing methanol. As shown in **Fig. 5(a)** and entry no. 3 of **Table 4**, a maximum of 95 % conversion of benzoin was achieved at the oxidant to substrate ratio of 3 : 1, after 4 h of reaction time. Lowering the amount of oxidant decreases the conversion. The effect of amount of catalyst on the oxidation of benzoin was studied considering two different amounts of  $[\text{MoO}_2\text{L}^1(\text{EtOH})]\cdot\text{EtOH}$  (**1**) viz. 0.0005 and 0.0015 g for the fixed amount of benzoin (1.06 g, 5 mmol) and 30%  $\text{H}_2\text{O}_2$  (1.7 g, 15 mmol) in 10 mL of methanol and reaction was monitored at reflux temperature of

methanol. **Fig. 5(b)** shows that maximum of 94 % conversion was achieved with 0.0005 g of catalyst. This conversion improved only marginally to 98% with 0.0015 g of catalyst. Thus only 0.0005 g of catalyst can be considered sufficient to optimize other reaction conditions. The amount of solvent also influences on the oxidation of benzoin. It was concluded (**Fig. 5(c)** and entry no. 6 and 7 of **Table 4**) that 10 mL methanol was sufficient to obtain maximum conversion under above optimized reaction conditions. **Table 4** summarizes different experimental conditions for the oxidation of benzoin. Thus, from these experiments, the best reaction conditions for the maximum oxidation of benzoin as concluded are: catalyst  $[\text{MoO}_2\text{L}^1(\text{EtOH})]\cdot\text{EtOH}$  (**1**) (0.0005 g), benzoin (1.06 g, 5 mmol) and 30%  $\text{H}_2\text{O}_2$  (1.7 g, 15 mmol) and refluxing methanol (10 mL).

**Fig. 5(d)** exhibits the selectivity of products along with the conversion of benzoin as a function of time (4 h) under the optimal experimental conditions as concluded above, *i.e.* benzoin (1.06 g, 5 mmol), 30%  $\text{H}_2\text{O}_2$  (1.7 g, 15 mmol),  $[\text{MoO}_2\text{L}^1(\text{EtOH})]\cdot\text{EtOH}$  (**1**) (0.0005 g) and methanol (10 mL) under reflux condition. It is clear from the plot that all products form with the conversion of benzoin. The highest selectivity of benzil (*ca.* 73.7%) was observed in the first one hour. With intervene of time, its selectivity slowly decreases and finally becomes almost constant and reaches 45 % after 4h. In the case of benzoic acid *ca.* 26.3% selectivity was found in first one hour which increases in next two hour and further decrease and reaches 39.4% in last hour. The selectivity of benzaldehyde-dimethylacetal increases continuously from 2.5 to 15.6 %. Thus, with the maximum benzoin oxidation of 94 % after 4 h of reaction time, the selectivity of the reaction products varies in the order: benzil(45%) > benzoic acid (39.4 %) > benzaldehyde-dimethylacetal (15.6 %).

Other catalysts were also tested under these reaction conditions and gave similar results.

**Table 5** provides turnover frequency (TOF) and selectivity details of products. It is clear

from the table that other complexes are also catalytically active and show equally good results with very high turnover frequency and the selectivity order of various products.

In one of our previous reports, where oxidomolybdenum(VI) complexes of similar ligands were employed as catalysts [32], it was found that during the catalytic oxidation of benzoin, a small amount of methylbenzoate was formed along with benzil, benzoic acid and benzaldehyde-dimethylacetal. Similar observations were also reported by Maurya et al. where dioxidomolybdenum(VI) complexes of tribasic pentadentate Schiff base ligands were used as catalysts [60]. In the present case, a bulky 3-hydroxy-2-naphthoic hydrazide was incorporated in the ligands of the reported oxidomolybdenum(VI) complexes (**1–7**). Interestingly when **1–7** was employed as catalysts, the formation of methylbenzoate could be avoided. Also the selectivity of formation of benzil now increased to 45% which was 15–16% in the previous reports. Kurapati et al. [63] have reported the catalysis of oxidation of benzoin with oxidomolybdenum(VI) complexes containing unsymmetrical tripodal NO<sub>3</sub> donor ligands where similar product selectivity was observed. However, it was reported that selectivity of formation of benzil was around 30% and the TOF was 125 h<sup>-1</sup>. In the present case, a better selectivity of benzil (45%) and TOF (1162–1468 h<sup>-1</sup>) was achieved.

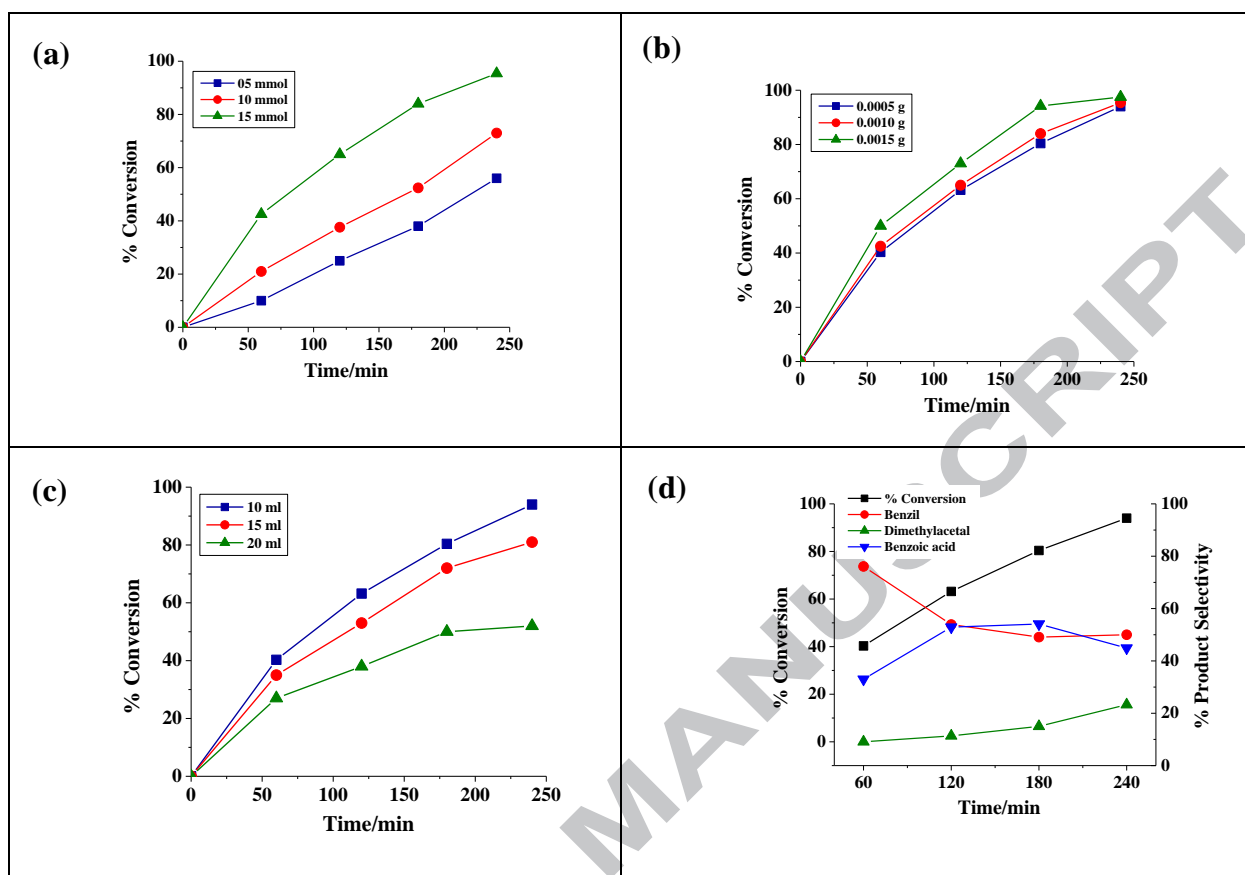


**Fig. 5.** (a) Effect of oxidant amount on the oxidation of benzoin. Reaction conditions: benzoin (1.06 g, 5 mmol), catalyst amount (0.0005 g) and methanol (10 ml). (b) Effect of catalyst amount on the oxidation of benzoin. Reaction conditions: benzoin (1.06 g, 5 mmol), 30 %  $\text{H}_2\text{O}_2$  (1.7 g, 15 mmol) and methanol (10 ml). (c) Effect of solvent amount on the oxidation of benzoin. Reaction conditions: benzoin (1.06 g, 5 mmol), catalyst amount (0.0005 g) and 30%  $\text{H}_2\text{O}_2$  (1.7 g, 15 mmol). (d) Plot showing percentage conversion of benzoin and the selectivity of benzoic acid, benzaldehyde, dimethylacetal and benzil formation as a function of time.

**Table 4** Conversion of benzoin (1.06 g, 5 mmol) using  $[\text{MoO}_2\text{L}^1(\text{EtOH})]\cdot\text{EtOH}$  (**1**) as catalyst in 4 h of reaction time under different reaction conditions.<sup>a</sup>

Entry No.	Catalyst (g)	H <sub>2</sub> O <sub>2</sub> (g, mmol)	CH <sub>3</sub> OH (ml)	Conversion %
1	0.0010	0.57, 05	10	56
2	0.0010	1.14, 10	10	73
3	0.0010	1.71, 15	10	95
4	0.0005	1.71, 15	10	94
5	0.0015	1.71, 15	10	98
6	0.0005	1.71, 15	15	81
7	0.0005	1.71, 15	20	52

<sup>a</sup> In the trial experiments, the catalytic efficiencies were also tested taking lower amounts of catalysts but the observed percent conversion was relatively low.

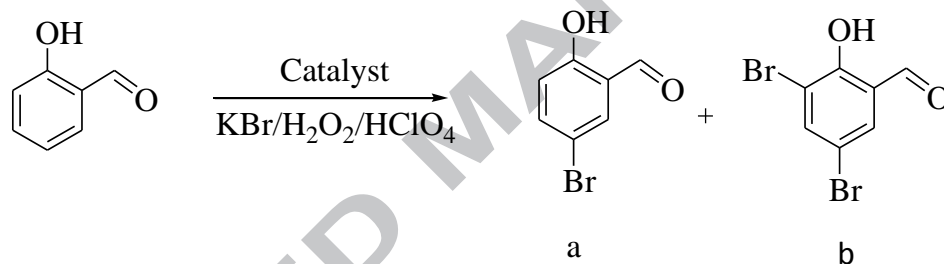
**Table 5** Effect of different catalysts on the oxidation of benzoin, TOF and product selectivity.

Catalyst (g)	TOF (h <sup>-1</sup> )	Conversion (%)	Selectivity (%) <sup>a</sup>		
			a	b	c
<b>1</b>	1175	94	45	15.6	39.4
<b>2</b>	1347	97	50	13.2	36.8
<b>3</b>	1468	94	50	15.5	34.5
<b>4</b>	1468	94	49	15.4	35.6
<b>5</b>	1162	93	45.7	8.4	45.9
<b>6</b>	1305	94	45.4	16.6	38
<b>7</b>	1333	96	49.8	10.2	40

<sup>a</sup> (a) benzil, (b) benzaldehyde-dimethyl acetal and (c) benzoic acid.

### 3.6.2. Oxidative bromination of salicylaldehyde

We have also found that the dioxidomolybdenum(VI) complexes effectively catalyze the oxidative bromination of salicylaldehyde to give 5-bromosalicylaldehyde and 3,5-dibromosalicylaldehyde using  $\text{H}_2\text{O}_2/\text{KBr}$  in the presence of  $\text{HClO}_4$  in aqueous solution at room temperature. In oxidative bromination reactions,  $\text{HOBr}$  is reported as an active species which is catalytically generated by the reaction of metal complex with  $\text{KBr}$  in the presence of  $\text{H}_2\text{O}_2$  and  $\text{HClO}_4$ . It reacts with organic substrates and converts them into final brominated products (**Scheme 3**) [107].



**Scheme 3.** Brominated products of Salicylaldehyde (a) 5-bromosalicylaldehyde, (b) 3,5-dibromosalicylaldehyde

In order to achieve optimum reaction conditions, several parameters like amount of  $\text{HClO}_4$ , amount of catalyst, amount of oxidant and amount of  $\text{KBr}$  were studied. Maximum conversion of salicylaldehyde was obtained with salicylaldehyde (0.610 g, 5 mmol),  $\text{KBr}$  (1.785 g, 15 mmol), aqueous 30%  $\text{H}_2\text{O}_2$  (1.71 g, 15 mmol), catalyst (0.0010 g), aqueous 70%  $\text{HClO}_4$  (2.14 g, 15mmol) and water (20 mL) in 2h. The complexes slowly decompose during the reaction on addition of greater amount of  $\text{HClO}_4$ . To avoid this decomposition of the catalyst  $\text{HClO}_4$  was added successfully in four equal portions. At least two products were identified under the above best suitable reaction condition with a maximum of 91% conversion using  $[\text{MoO}_2\text{L}^1(\text{EtOH})]\cdot\text{EtOH}$  (**1**) as catalyst (**Table 6**). Increasing the amount of

oxidant improves the conversion of salicylaldehyde. The presence of an excess of  $\text{H}_2\text{O}_2$  facilitates the formation of more and more HOBr which ultimately helps in the further oxidative bromination of salicylaldehyde to the other position(s). Other catalysts gave similar conversion and selectivity order of products and the results obtained are summarized in **Table 7**. In the absence of the catalyst, the reaction mixture gave only *ca.* 35% conversion of salicylaldehyde.

Comparing the obtained results with our previous report [32], it was found that 5-bromosalicylaldehyde and 3,5-dibromosalicylaldehyde was formed selectively when **1–7** were used as catalysts and a third product 2,4,6-tribromophenol was not formed, as reported earlier [32,82]. Also the selectivity of 5-bromosalicylaldehyde has increased to 87.6–92.8 % in the present case, while in the earlier case it was around 56.5–75%. The TOF (1107–1382  $\text{h}^{-1}$ ) was comparable to the previous report. A higher TOF (3840–3920  $\text{h}^{-1}$ ) was reported by Kurapati et al. [83] for the oxidative bromination of salicylaldehyde catalyzed by oxidomolybdenum(VI) complexes, however the selectivity of the 5-bromosalicylaldehyde was better in the present case than the reported work by Kurapati et al. [83].

**Table 6** Results of oxidative bromination of salicylaldehyde(0.610, 5 mmol) catalyzed by  $[\text{MoO}_2\text{L}^1(\text{EtOH})]\cdot\text{EtOH}$  (**1**) after 2 h of contact time.<sup>a</sup>

Entry no.	Catalyst(g)	H <sub>2</sub> O <sub>2</sub> (g, mmol)	KBr (g, mmol)	HClO <sub>4</sub> (g, mmol)	Conversion %
1	0.0005	1.14,10	1.19,10	1.43, 10	35
2	0.0010	1.14,10	1.19, 10	1.43, 10	42
3	0.0015	1.14, 10	1.19, 10	1.43, 10	45
4	0.0010	1.71, 15	1.19, 10	1.43, 10	64
5	0.0010	2.27, 20	1.19,10	1.43, 10	72
6	0.0010	1.71, 15	1.78, 15	1.43, 10	84
7	0.0010	1.71, 15	2.38, 20	1.43, 10	88
8	0.0010	1.71, 15	1.78, 15	2.14, 15	91
9	0.0010	1.71, 15	1.78, 15	2.86, 20	94

<sup>a</sup>In the trial experiments, the catalytic efficiencies were also tested taking lower amounts of catalysts but the observed percent conversion was relatively low.

**Table 7** Effect of different catalysts on the oxidative bromination of salicylaldehyde, TOF and product selectivity.

Catalyst (g)	TOF(h <sup>-1</sup> )	Conversion (%)	Selectivity (%)	
			monobromo	Dibromo
<b>1</b>	1138	91	90.3	9.7
<b>2</b>	1223	93	87.6	12.4
<b>3</b>	1352	92	89.5	10.5
<b>4</b>	1382	94	91.0	9.0
<b>5</b>	1107	93	92.8	7.2
<b>6</b>	1223	93	90.6	9.4
<b>7</b>	1210	92	91.0	9.0

### 3.6.3. Reactivity of complexes with H<sub>2</sub>O<sub>2</sub>

As accounted previously, dioxidomolybdenum(VI) complexes on reaction with H<sub>2</sub>O<sub>2</sub> give the corresponding [Mo<sup>VI</sup>O(O<sub>2</sub>)<sup>2+</sup>] complexes [108]. Such species has been generated in DMSO and the progress of reaction has been monitored by electronic absorption spectroscopy. The stepwise additions of H<sub>2</sub>O<sub>2</sub> (1.35 g, 12mmol) dissolved in 5 mL of DMSO to 20 mL of ca. 4 × 10<sup>-5</sup> M solution of [MoO<sub>2</sub>L<sup>1</sup>(EtOH)].EtOH (**1**) in DMSO causes the decrease in intensities of the 410 and 330 nm bands (**Fig. 6**). The decrement in the band at 410 nm, occurs due to the ligand to metal charge transfer transition and shows the formation of oxidoperoxidomolybdenum moiety. Simultaneously the one UV band appearing at 263 nm experiences a considerable increase in intensity.

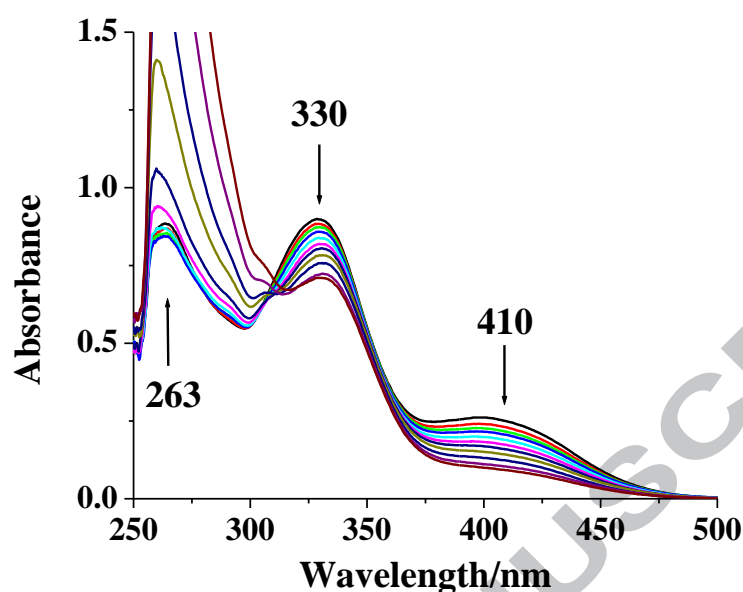
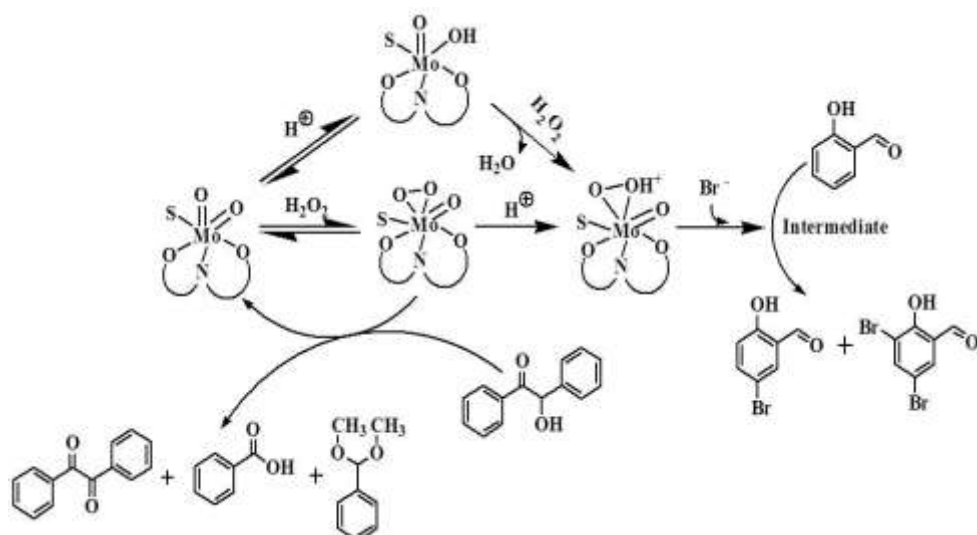


**Fig. 6.** UV–Vis spectral changes observed during titration of **1** with H<sub>2</sub>O<sub>2</sub>. The spectra were recorded after consecutive additions of drops of 30% H<sub>2</sub>O<sub>2</sub> (12mmol) dissolved in 5 mL of DMSO to 20 mL of  $4 \times 10^{-5}$  M solution in DMSO.

The exact mechanism for oxidation of benzoin and oxidative bromination of salicylaldehyde by oxidometal complexes in the presence of H<sub>2</sub>O<sub>2</sub> is not clear at present. The formation of relevant oxido-peroxido complexes has been reported in the past [109,110]. Although no attempts to isolate the appropriate intermediates for this system have been performed, based on the oxidation products obtained and experiments described above, a reaction pathway including oxido-peroxido intermediates can be rationally proposed (**Scheme 4**).



**Scheme 4.** Catalytic mechanism for the oxidative bromination of salicylaldehyde and oxidation of benzoin. [where S = EtOH/DMSO]

#### 4. Conclusions

In summary, this article presents the synthesis and characterization of seven new dioxidomolybdenum(VI) complexes (**1–7**) of aroylazines and sheds light on their catalytic potential. The structures of **1–6** have been established by single crystal X-ray crystallography. The catalytic activity of **1–7** has been tested for oxidation of benzoin and oxidative bromination of salicylaldehyde. In all the cases the percentage of conversion is increased significantly in the presence of catalysts and show high a percentage of conversion (>90%) with a high turnover frequency (>1100 h<sup>-1</sup>). The catalytic mechanism for oxidation of benzoin and oxidative bromination of salicylaldehyde by dioxidomolybdenum(VI) complexes has also been proposed and the intermediate oxidoperoxido species, expected to be involved in catalysis, has also been generated from a solution of **1** and studied by UV-vis spectroscopy. From the comparison of the obtained data with previous reports [32,60,63,82,83], it can be concluded that, introduction of the bulky [32] 3-hydroxy-2-naphthoic substituent in the complexes **1–7**, increases their catalytic activity both in terms of selectivity and turnover frequency than previously reported catalysts. The complexes **1–7** are good catalyst precursors for the oxidative bromination of salicylaldehyde in the presence of green oxidant 30% H<sub>2</sub>O<sub>2</sub>, HClO<sub>4</sub> and bromide ion, and therefore acts as functional models of vanadium dependent haloperoxidases. Complex **4**, which contained two bulky naphthyl groups, exhibited the maximum % conversion of products (94%) and TOF (1382 h<sup>-1</sup>) in the oxidative bromination of salicylaldehyde. In view of the above results, it can be predicted that the dioxidomolybdenum(VI) complexes under study may have the potential to stimulate research for the synthesis of a better catalyst.

**Acknowledgement**

Funding for this research was provided by Council of Scientific and Industrial Research, Government of India [Grant No. 01(2735)/13/EMR-II].

**Appendix A. Supplementary data**

CCDC contains the supplementary crystallographic data for **1–6**. These data can be obtained free of charge via <http://www.ccdc.cam.ac.uk/conts/retrieving.html>, or from the Cambridge Crystallographic Data Centre, 12 Union Road, Cambridge CB2 1EZ, UK; fax: +44 1223 336 033; or e-mail: [deposit@ccdc.cam.ac.uk](mailto:deposit@ccdc.cam.ac.uk). Supplementary data associated with this article can be found, in the online version, at DOI: XXXXX

**Corresponding Author**

E-mail: [rupamdinda@nitrrkl.ac.in](mailto:rupamdinda@nitrrkl.ac.in) (R. Dinda)

Tel.: + (91) 661 246 2657; Fax: + (91) 661 246 2022

**References**

- [1] M. Amini, M.M. Haghdoost, M. Bagherzadeh, *Coord. Chem. Rev.* 257 (2013) 1093–1121.
- [2] R.D. Chakravarthy, D.K. Chand, *J. Chem. Sci.* 123 (2011) 187–199.
- [3] K. Heinze, *Coord. Chem. Rev.* 300 (2015) 121–141.
- [4] R. Hille, *Chem. Rev.* 96 (1996) 2757–2816.
- [5] D. Collison, C.D. Garner, J.A. Joule, *Chem. Soc. Rev.* 25 (1996) 25–32.
- [6] A. Sigel, H. Sigel (Eds.), *Metal Ions in Biological Systems 39, Molybdenum and Tungsten, Their Roles in Biological Processes*, Marcel Dekker, New York, 2002.
- [7] R.C. Bray, B. Adams, A.T. Smith, B. Bennett, S. Bailey, *Biochemistry*, 39 (2000) 11258– 11269.
- [8] K. Jeyakumar, D.K. Chand, *J. Chem. Sci.* 121 (2009) 111–123.
- [9] T. Punniyamurthy, S. Velusamy, J. Iqbal, *Chem. Rev.* 105 (2005) 2329– 2363.
- [10] F.E. Kühn, A.M. Santos, M. Abrantes, *Chem. Rev.* 106 (2006) 2455–2475.
- [11] S. Roberto, R.P. Maria, *Curr. Org. Synth.* 6 (2009) 239–263.
- [12] A. Syamal, M.R. Maurya, *Coord. Chem. Rev.* 95 (1989) 183–238.
- [13] A.L. Tenderholt, K.O. Hodgson, B. Hedman, R.H. Holm, E.I. Solomon, *Inorg. Chem.* 51 (2012) 3436– 3442.
- [14] R. Hille, *Trends Biochem. Sci.* 27 (2002) 360–367.
- [15] J.H. Enemark, J.J.A. Cooney, J.-J. Wang, R.H. Holm, *Chem. Rev.* 104 (2004) 1175–1200.
- [16] G. Romanowski, J. Kira, *Polyhedron* 117 (2016) 352–358.
- [17] M. Bagherzadeh, M. Amini, H. Parastar, M. Jalali-Heravi, A. Ellern, L.K. Woo, *Inorg. Chem. Commun.* 20 (2012) 86–89.

- [18] M. Cindric, G. Pavlovic, R. Katava, D. Agustin, *New J. Chem.* 41 (2017) 594–602.
- [19] A. Rezaeifard, I. Sheikhshoae, N. Monadi, H. Stoeckli-Evans, *Eur. J. Inorg. Chem.* (2010) 799–806.
- [20] A. Lehtonen, M. Wasberg, R. Sillanpää, *Polyhedron* 25 (2006) 767–775.
- [21] J.A. M. Brandts, J. Boersma, A.L. Spek, G. van Koten, *Eur. J. Inorg. Chem.* (1999) 1727–1733.
- [22] N. Zwettler, M.E. Judmaier, L. Strohmeier, F. Belaj, N.C. Mosch-Zanetti, *Dalton Trans.* 45 (2016) 14549–14560.
- [23] W. Fan, Y. Leng, J. Liu, P. Jiang, J. Zhao, *Appl. Catal. A*, 506 (2015) 173–179.
- [24] S.K. Kurapati, S. Pal, *Dalton Trans.* 44 (2015) 2401–2408.
- [25] M.E. Judmaier, C. Holzer, M. Volpe, N.C. Mösch-Zanetti, *Inorg. Chem.* 51 (2012) 9956–9966.
- [26] A. Rezaeifard, I. Sheikhshoae, N. Monadi, H. Stoeckli-Evans, *Eur. J. Inorg. Chem.* (2010) 799–806.
- [27] S.P. Dash, S. Majumder, A. Banerjee, M.F.N.N. Carvalho, P. Adão, J. Costa Pessoa, K. Brzezinski, E. Garribba, H. Reuter, R. Dinda, *Inorg. Chem.* 55 (2016) 1165–1182.
- [28] S.P. Dash, S. Roy, M. Mohanty, M.F.N.N. Carvalho, M.L. Kuznetsov, J.C. Pessoa, A. Kumar, Y.P. Patil, A. Crochet, R. Dinda, *Inorg. Chem.* 55 (2016) 8407–8421.
- [29] M. Mancka, W. Plass, *Inorg. Chem. Commun.* 10 (2007) 677–680.
- [30] S.P. Dash, S. Pasayat, S. Bhakat, S. Roy, R. Dinda, E.R.T. Tiekink, S. Mukhopadhyay, S.K. Bhutia, M.R. Hardikar, B.N. Joshi, Y.P. Patil, M. Nethaji, *Inorg. Chem.* 52 (2013) 14096–14107.
- [31] S. Naskar, M. Corbella, A.J. Blake, S.K. Chattopadhyay, *Dalton Trans.* (2007) 1150–1159.

- [32] S. Pasayat, S.P. Dash, S. Roy, R. Dinda, S. Dhaka, M.R. Maurya, W. Kaminsky, Y.P. Patil, M. Nethaji, *Polyhedron* 67 (2014) 1–10.
- [33] C.–Y. Hsu, H. –C. Tseng, J.K. Vandavasi, W.–Y. Lu, L.–F. Wang, M. Y. Chiang, Y. – C. Lai, H.–Y. Chen, H.–Y. Chen, *RSC Adv.* 7 (2017) 18851– 18860.
- [34] A. Li, Haiyan Ma and J. Huang, *Appl. Organometal. Chem.* 27 (2013) 341–347.
- [35] H. Hamaki, N. Takeda, M. Nabika, N. Tokitoh, *Macromolecules* 45 (2012) 1758–1769.
- [36] M.R. Maurya, *Curr. Org. Chem.* 16 (2012) 73–88.
- [37] W. Plass, *Z. Anorg. Allg. Chem.* 623 (1997) 997–1005.
- [38] A.J. Burke, *Coord. Chem. Rev.* 252 (2008) 170–175.
- [39] K.R. Jain, W.A. Herrmann, F.E. Kuhn, *Coord. Chem. Rev.* 252 (2008) 556–568.
- [40] K.C. Gupta, A.K. Sutar, *Coord. Chem. Rev.* 252 (2008) 1420–1450.
- [41] B. Frédéric, *Coord. Chem. Rev.* 236 (2003) 71–89.
- [42] R.R. Schrock, *J. Mol. Catal. A: Chem.* 213 (2004) 21–30.
- [43] K. Most, J. Hoßbach, D. Vidović, J. Magull, N.C. Mösch-Zanetti, *Adv. Synth. Catal.* 347 (2005) 463–472.
- [44] M.K. Hossain, M. Haukka, R. Sillanpaa, D.A. Hrovat, M.G. Richmond, E. Nordlander, A. Lehtonen, *Dalton Trans.* 46 (2017) 7051–7060.
- [45] G. Mohammadnezhad, R. Debel, W. Plass, *J. Mol. Catal. A: Chem.* 410 (2015) 160–167.
- [46] B.E. Schultz, S.F. Gheller, M.C. Muetterties, M.J. Scott, R.H. Holm, *J. Am. Chem. Soc.* 115 (1993) 2714–2722.
- [47] Y. Brussaard, F. Olbrich and E. Schaumann, *Inorg. Chem.* 52 (2013) 13160–13166.
- [48] R.A. Sheldon, J.K. Kochi, *Metal Catalyzed Oxidations of Organic Compounds*, Academic Press, New York, 1981.
- [49] B.M. Trost, I. Fleming, S.V. Ley (Eds.), *Comprehensive Organic Synthesis*, Pergamon, Oxford, 7, 1991, 251.

- [50] H. Morrison, S. Danishefsky, P. Yates, *J. Org. Chem.* 26 (1961) 2617–2618.
- [51] K.P.C. Vollhardt, N.E. Schore, *Organic Chemistry*, 2nd edn. Freeman, New York (1994) 924.
- [52] A. Kumar Mitra, A. De, N. Karchaudhuri, *J. Chem. Res. (S)*, (1999) 246–247.
- [53] J.D. Lou, L. Li, N. Vatanian, X.L. Lu, X. Yu, *Synth. React. Inorg., Met.-Org. Chem.*, 38 (2008) 373–375.
- [54] D. Pagoria, A. Lee, W. Geurtsen, *Biomaterials*, 26 (2005) 4091–4099.
- [55] G. Cainelli, G. Cardillo, *Chromium Oxidation in Organic Chemistry*, Springer, Berlin, 1984.
- [56] J.S. Buck, S.S. Jenkins, *J. Am. Chem. Soc.* 51 (1929) 2163–2167.
- [57] M. Weiss, M. Appel, *J. Am. Chem. Soc.* 70 (1948) 3666–3667.
- [58] A. McKillop, B.P. Swann, M.E. Ford, E.C. Taylor, *J. Am. Chem. Soc.* 95 (1973) 3641–3645.
- [59] S. Yasuike, Y. Kishi, S. Kawara, J. Kurita, *Chem. Pharm. Bull.* 53 (2005) 425–427.
- [60] M.R. Maurya, S. Dhaka, F. Avecilla, *Polyhedron*, 67 (2014) 145–159.
- [61] N. Ueyama, N. Yoshinaga, A. Nakamura, *J. Chem. Soc., Dalton Trans.* (1990) 387–394.
- [62] R.K. Bhatia, G.N. Rao, *J. Mol. Catal. A: Chem.* 121 (1997) 171–178.
- [63] S.K. Kurapati, S. Maloth, S. Pal, *Inorg. Chim. Acta*, 430 (2015) 66–73.
- [64] M.C.R. Franssen, *Catal. Today*, 22 (1994) 441–458.
- [65] A. Butler, M. Sandy, *Nature* 460 (2009) 848–854.
- [66] C. Leblanc, H. Vilter, J.B. Fournier, L. Delage, P. Potin, E. Rebuffet, G. Michel, P.L. Solari, M.C. Feiters, M. Czjzek, *Coord. Chem. Rev.* 301–302 (2015) 134–146.
- [67] M.R. Maurya, *J. Chem. Sci.* 118 (2006) 503–511.
- [68] W. Plass, *Angew. Chem. Int. Ed.* 38 (1999) 909–912.

- [69] S.L. Neidleman, *Biohalogenation: Principles, Basic Roles and Applications*, Halsted Press, New York, 1986.
- [70] J.N. Carter-Franklin, A. Butler, *J. Am. Chem. Soc.* 126 (2004) 15060–15066.
- [71] A. Butler, J.N. Carter-Franklin, *Nat. Prod. Rep.* 21 (2004) 180–188.
- [72] D. Lahaye, J.T. Groves, *J. Inorg. Biochem.* 101 (2007) 1786–1797.
- [73] A. Butler, J.V. Walker, *Chem. Rev.* 93 (1993) 1937–1944.
- [74] R. Wever, M.A. van der Horst, *Dalton Trans.* 42, 2013, 11778–11786.
- [75] A.G.J. Ligtenbarg, R. Hage, B.L. Feringa, *Coord. Chem. Rev.* 237 (2003) 89–101.
- [76] D. Wischang, O. Brücher, J. Hartung, *Coord. Chem. Rev.* 255 (2011) 2204–2217.
- [77] K. Kikushima, T. Moriuchi, T. Hirao, *Tetrahedron* 66 (2010) 6906–6911.
- [78] X.-a. Zhang, W.-D. Woggon, *J. Am. Chem. Soc.* 127 (2005) 14138–14139.
- [79] I. Lippold, H. Görls, W. Plass, *Eur. J. Inorg. Chem.* 2007 (2007) 1487–1491.
- [80] A. Pohlmann, S. Nica, T.K.K. Luong, W. Plass, *Inorg. Chem. Commun.* 8 (2005) 289–292.
- [81] W. Plass, *Pure. Appl. Chem.* 81 (2009) 1229–1239.
- [82] M.R. Maurya, N. Kumar, F. Avecilla, *J. Mol. Catal. A: Chem.* 392 (2014) 50–60.
- [83] S.K. Kurapati, S. Pal, *Appl. Organometal. Chem.* 30 (2016) 116–124.
- [84] S.P. Dash, A.K. Panda, S. Dhaka, S. Pasayat, A. Biswas, M.R. Maurya, P.K. Majhi, A. Crochet, R. Dinda, *Dalton Trans.* 45 (2016) 18292–8307.
- [85] S.P. Dash, A.K. Panda, S. Pasayat, R. Dinda, A. Biswas, E.R.T. Tiekink, S. Mukhopadhyay, S.K. Bhutia, W. Kaminsky, E. Sinn, *RSC Adv.* 5 (2015) 51852–51867.
- [86] Saswati, A. Chakraborty, S.P. Dash, A.K. Panda, R. Acharyya, A. Biswas, S. Mukhopadhyay, S.K. Bhutia, A. Crochet, Y.P. Patil, M. Nethaji, R. Dinda, *Dalton Trans.* 44 (2015) 6140–6157.

- [87] S.P. Dash, A.K. Panda, S. Pasayat, S. Majumder, A. Biswas, W. Kaminsky, S. Mukhopadhyay, S.K. Bhutia, R. Dinda, *J. Inorg. Biochem.* 144 (2015) 1–12.
- [88] S.P. Dash, A.K. Panda, S. Pasayat, R. Dinda, A. Biswas, E.R.T. Tiekink, Y.P. Patil, M. Nethaji, W. Kaminsky, S. Mukhopadhyay, S.K. Bhutia, *Dalton Trans.* 43 (2014) 10139–10156.
- [89] S. Pasayat, S.P. Dash, S. Majumder, R. Dinda, E. Sinn, H. Stoeckli-Evans, S. Mukhopadhyay, S.K. Bhutia, P. Mitra, *Polyhedron* 80 (2014) 198–205.
- [90] Saswati, R. Dinda, C.S. Schmiesing, E. Sinn, Y.P. Patil, M. Nethaji, H. Stoeckli-Evans and R. Acharyya, *Polyhedron* 50 (2013) 354–363.
- [91] S. Pasayat, S.P. Dash, Saswati, P.K. Majhi, Y.P. Patil, M. Nethaji, H.R. Dash, S. Das, R. Dinda, *Polyhedron* 38 (2012) 198–204.
- [92] S.P. Dash, S. Pasayat, Saswati, H.R. Dash, S. Das, R.J. Butcher and R. Dinda, *Polyhedron* 31 (2012) 524–529.
- [93] S. Pasayat, M. Böhme, S. Dhaka, S.P. Dash, S. Majumder, M.R. Maurya, W. Plass, W. Kaminsky, R. Dinda, *Eur. J. Inorg. Chem.* (2016) 1604–1618.
- [94] G.J.-J. Chen, J.W. McDonald and W.E. Newton, *Inorg. Chem.* 15 (1976) 2612–2615.
- [95] Bruker, APEX 2 - Suite of Crystallographic Software. (2008) Madison, Wisconsin, USA.
- [96] SAINT. (2008) Bruker AXS Inc.: Madison, Wisconsin, USA.
- [97] SADABS. (2008) Bruker AXS Inc.: Madison, Wisconsin, USA.
- [98] T. Hahn, ed. *International Tables for Crystallography* 4th ed. Vol. A Space-Group Symmetry. (1996) Kluwer Academic Publishers: Dordrecht.
- [99] G.M. Sheldrick, *Acta Cryst.* 64 (2008) 112–122.
- [100] A.J.C. Wilson, ed. *International Tables for Crystallography*. Kluwer Academic Publishers: Dordrecht, Vol. C. (1992).

- [101] K. Brandenburg, *Diamond - Crystal and Molecular Visualization*. Crystal Impact: Bonn, Germany (2006).
- [102] C.F. Macrae, I.J. Bruno, J.A. Chisholm, P.R. Edgington, P. McCabe, E. Pidcock, L. Rodriguez-Monge, R. Taylor, J. van de Streek, P.A. Wood, *Appl. Crystallogr.* 41 (2008) 466–470.
- [103] R. Dinda, P. Sengupta, S. Ghosh, H.M. Figge, W.S. Sheldrick, *Dalton Trans.* (2002) 4434–4439.
- [104] R. Dinda, P. Sengupta, S. Ghosh, W.S. Sheldrick, *Eur. J. Inorg. Chem.* 2003, 363–369.
- [105] S.F. Gheller, W.E. Newton, L.P. de Majid, J.R. Bradbury, F.A. Schultz, *Inorg. Chem.* 27 (1988) 359–366.
- [106] M.R. Maurya, C. Haldar, A. Kumar, M.L. Kuznetsov, F. Avecilla, J. Costa Pessoa, *Dalton Trans.* 42 (2013) 11941–11962.
- [107] G.B. Gill, in *Comprehensive Organic Synthesis*, ed. G. Pattenden, vol. 3, Pergamon Press, New York (1991) 821.
- [108] M.R. Maurya, N. Kumar, F. Avecilla, *J. Mol. Catal. A: Chem.* 392 (2014) 50–60.
- [109] S. Nica, A. Pohlmann, W. Plass, *Eur. J. Inorg. Chem.* (2005) 2032–2036.
- [110] S.K. Maiti, S. Dinda, N. Gharah, R. Bhattacharyya, *New J. Chem.* 30 (2006) 479–489.

- Sterically constrained aroylazine ligands
- *cis*-Dioxidomolybdenum(VI) complexes
- X-Ray Crystallography
- Catalytic applications on oxidation of benzoin and oxidative bromination of salicylaldehyde

ACCEPTED MANUSCRIPT

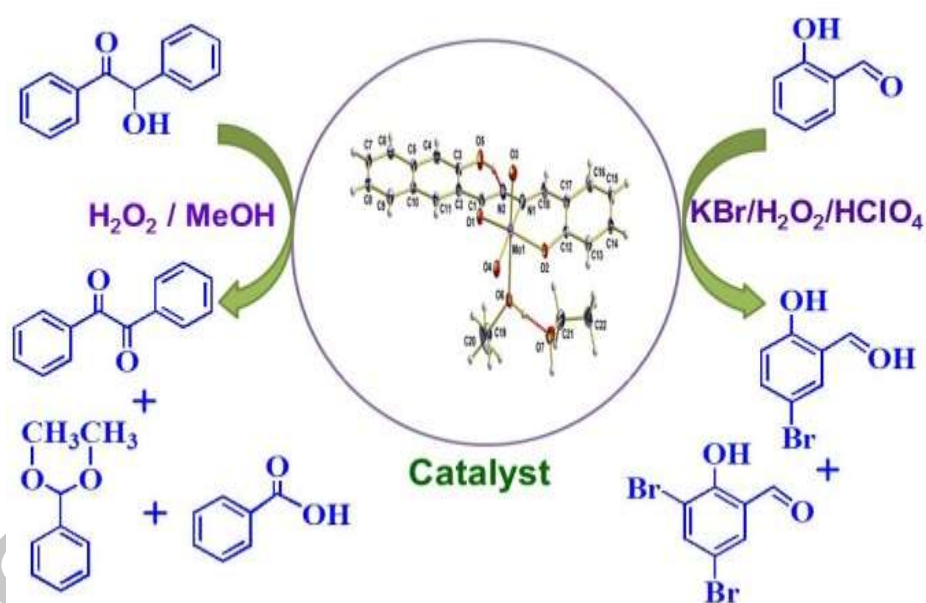
## Graphical Abstract for Table of content

**Dioxidomolybdenum(VI) complexes bearing sterically constrained aroylazine ligands:**

**Synthesis, structural investigation and catalytic evaluation**

Sudarshana Majumder, Sagarika Pasayat, Satabdi Roy, Subhashree P. Dash, Sarita Dhaka,

Mannar R. Maurya, Martin Reichelt, Hans Reuter, Krzysztof Brzezinski and Rupam Dinda



**Textual Abstract for Table of content**

**Dioxidomolybdenum(VI) complexes bearing sterically constrained aroylazine ligands:  
Synthesis, structural investigation and catalytic evaluation**

Sudarshana Majumder, Sagarika Pasayat, Satabdi Roy, Subhashree P. Dash, Sarita Dhaka,  
Mannar R. Maurya, Martin Reichelt, Hans Reuter, Krzysztof Brzezinski and Rupam Dinda

Synthesis, characterization and catalytic potential of dioxidomolybdenum (VI) complexes of aroylazines.

ACCEPTED MANUSCRIPT